Electrical Networks and Algebraic Graph Theory: Models, Properties, and Applications

Florian Dörfler, *Member, IEEE,* John W. Simpson-Porco, *Member, IEEE,* and Francesco Bullo, *Fellow, IEEE*

***Abstract*—Algebraic graph theory is a cornerstone in the study of electrical networks ranging from miniature integrated circuits to continental-scale power systems. Conversely, many fundamental results of algebraic graph theory were laid out by early electrical circuit analysts. In this paper we survey some fundamental and historic as well as recent results on how algebraic graph theory informs electrical network analysis, dynamics, and design. In particular, we review the algebraic and spectral properties of graph adjacency, Laplacian, incidence, and resistance matrices and how they relate to the analysis, network-reduction, and dynamics of certain classes of electrical networks. We study these relations for models of increasing complexity ranging from static resistive DC circuits, over dynamic RLC circuits, to nonlinear AC power flow. We conclude this paper by presenting a set of fundamental open questions at the intersection of algebraic graph theory and electrical networks.**

I. Introduction

The study of electrical networks, the theory of graphs, and their associated matrices share a long and rich history of synergy and joint development. Starting from the foundational classical work by Gustav Kirchhoff [87], modeling and analysis of electric circuits has motivated the birth and the development of a broad range of graph-theoretical concepts and certain classes of matrices. Vice-versa, algebraic graph theory concepts and constructions have enabled fundamental advances in the theory of electrical networks. As is well known, it is in graph-theoretical language that Kirchhoff's laws are most succinctly and powerfully expressed, and it is via matrix theory that the discrete nature of graphs is most powerfully analyzed. To this day, graph theory, matrix analysis, and electrical networks inspire and enrich one another.

In this paper we survey some fundamental and historic as well as recent results on how algebraic graph theory informs electrical network analysis, dynamics, and design. In particular, we review the algebraic and spectral properties of graph adjacency, Laplacian, Metzler, incidence, and effective resistance matrices; we review the basic notions from algebraic potential theory, including cycle and cutset spaces.

F. Dörfler is with the Automatic Control Laboratory, ETH Zürich, 8092 Zürich, Switzerland. Email: dorfler@ethz.ch.

J. W. Simpson-Porco is with the Department of Electrical and Computer Engineering, University of Waterloo, Waterloo, ON N2L 3G1, Canada. Email: jwsimpson@uwaterloo.ca.

F. Bullo is with the Center for Control, Dynamical Systems and Computation, University of California, Santa Barbara, CA 93106, USA. Email: bullo@engineering.ucsb.edu.

This work was supported in part by the SNF AP Energy Grant #160573, the U.S. Department of Energy (DOE) Solar Energy Technologies Office under Contract No. DE-EE0000-1583, by the National Science and Engineering Council of Canada Discovery RGPIN-2017-04008, and by ETH Zürich funds.

We then study general models of electrical networks, starting from elementary models and building up to a prototypical circuit, with several instructive special cases. Our proposed prototypical circuit is a Π-line-coupled RC circuit with nonlinear sources and loads. This prototypical nonlinear RLC circuit has numerous interesting features. First, our prototypical circuit generalizes the widely-studied resistive circuit and features rich dynamical behaviors, including synchronization and consensus behaviors. Second, power system network modelling is essentially based on this circuit (Π-line transmission models, charging capacitors at the buses, and ZIP loads, including modern constant-power devices). Third and final, it showcases popular energy-based, power-based, and compartmental modeling approaches, and it is sufficiently general to admit a variety of graph-theoretic analysis approaches.

Based on algebraic graph theory methods, we then study the analysis, network-reduction, and dynamics of our prototypical circuit and its variations, in linear and nonlinear as well as static and dynamic settings. Thereby we consider models of increasing complexity ranging from static resistive circuits, over dynamic RLC networks, to nonlinear AC power flow models. We motivate our treatment with a few interesting examples, review a few fundamental and historic results in a tutorial exposition, and also showcase related recent developments. Our focus is on static and dynamic analysis of DC circuits, except for Section VI-B where we explicitly focus on steady-state analysis of AC circuits through the lens of graph theory.

It is important to clarify that this article does not aim to be comprehensive in its scope, nor does it present multiple viewpoints on the given material, as both algebraic graph theory and electrical circuits are mature and broadly developed fields. In the context of algebraic graph theory, we refer interested readers to the textbooks [16], [19], [72] and, for example, the surveys [102], [97], [17]. There are numerous complementary viewpoints on electrical network modeling and analysis. We mention the well-established linear network theory [6], [144], [101], [145]; classical network analysis in the nonlinear setting [37], [36], [124]; the signals, systems, and control viewpoint [4]; the behavioral approach [148] and its application to circuits [149]; energy-based Port-Hamiltonian approaches [135], [104], [133], [95]; and power-based Brayton-Moser approaches [25], [26], [83], [85], [84] among others. Our exposition and treatment highlights the algebraic graph theory perspective on electrical networks, with examples colored by our own research interests and experiences.

The remainder of the paper is organized as follows. We begin with a set of motivating examples in Section II that outline the themes of the paper. Section III briefly reviews relevant results of algebraic theory. In Section IV we present the general modeling of electrical networks based on the language of graph theory and also introduce a prototypical network model that we will frequently revisit in the course of the paper. Section V showcases the tools of algebraic graph theory to analyze the structure and dynamics of linear electrical networks, and Section VI addresses the nonlinear case. Finally, Section VII concludes the paper and outlines a few open and worthwhile research directions at the intersection of electrical networks and algebraic graph theory.

II. Motivating examples

We begin by laying out a set of motivating examples with apparently complex behavior, whose analysis becomes crisp and clear by using the tools of algebraic graph theory. We will revisit each of these examples in the course of the paper.

A. Synchronization of resonant LC tanks

Consider the electrical network in Figure 1 consisting of identical resonant tank circuits interconnected through resistive branches. Each tank circuit consists of a parallel connection of an inductor and a capacitor with identical values of inductance $\ell > 0$ and capacitance $c > 0$.

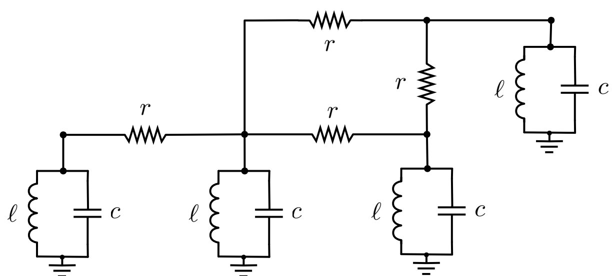

Fig. 1. Network of resistively interconnected ℓc-tanks; image courtesy of [27].

As known from undergraduate engineering education, each tank circuit in isolation exhibits harmonic oscillations with natural frequency $\omega_0 = 1/\sqrt{\ell c}$ and phase and amplitude depending on its initial conditions for current and voltages. When coupled through a connected resistive circuit, the voltages $v_i(t)$ across the capacitors of all tank circuits synchronize to a common harmonic oscillating voltage of frequency ω_0; see Figure 2 for a simulation. This *spontaneous* synchronization may appear either surprising or obvious to electrical engineers depending on their physical intuition. In Section V, we will show through the lens of algebraic graph theory that this effect is to be expected and can be analyzed at a similar complexity as the analysis of a single tank circuit.

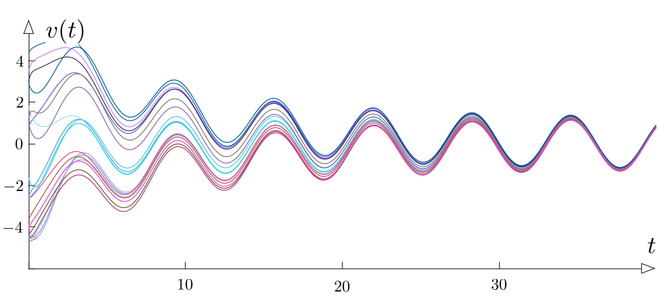

Fig. 2. Synchronization of capacitor voltages of the resistively interconnected identical tank circuits in Figure 1; image courtesy of [27].

B. RC circuits as compartmental systems

Consider the electrical network in Figure 3 consisting of resistive branches connecting capacitors with a current source and at least one so-called shunt resistor connected to ground.

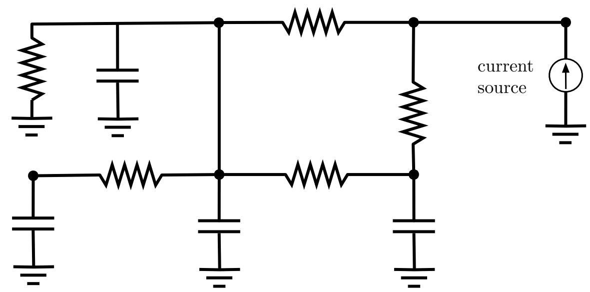

Fig. 3. Resistive network of capacitors with a current source and a shunt resistor.

It is possible and natural to model this dynamical system as a compartmental system, i.e., a collection of compartments in which electrical charge flows into the system through the current source, through the network, and out through the shunt resistor. In other words, in every compartment the stored, supplied, and dissipated charge is balanced.

The study of compartmental systems is rooted in algebraic graph theory; see Appendix A and [140], [79], [27]. A key result states that, if each node has a directed path to the shunt resistance, (i.e., the compartmental graph is out-flow connected), then the system has a unique, positive, globally asymptotically stable equilibrium point.

C. Steady-state feasibility of direct-current networks

Consider the DC circuit shown in Figure 4(a), which consists of an ideal DC voltage supply providing power to a load through a resistance r.

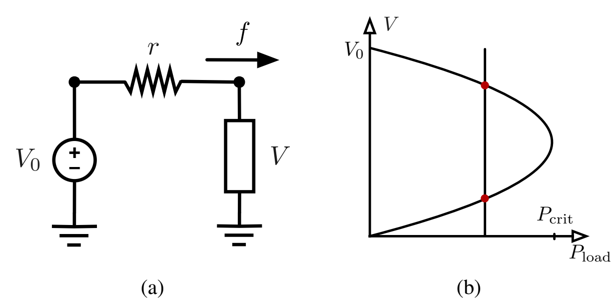

Fig. 4. (a) An ideal voltage supply connected to a nonlinear load. (b) Locus of solutions for constant-power load model.

The load consumes a power $P(V)$ as a function of the voltage V across its terminals. Since the current f which flows from the supply is $f = (V_0 - V)/r$, the load dissipates a power Vf. This must in turn equal its consumed power $P(V)$, yielding the power balance

$$V(V_0 - V)/r = P(V)\,. \tag{1}$$

This is a nonlinear equation in the load voltage V, the solutions of which will determine the feasible values for the voltage V. Let us first consider a resistive load of resistance $r_{\text{load}} > 0$, with power consumption $P(V) = V^2/r_{\text{load}}$. In this case, the power balance (1) always has two solutions, given by

$$V = 0 \qquad \text{and} \qquad V = \frac{r}{r + r_{\text{load}}} V_0\,.$$

Now, instead, consider a load consuming a constant power $P(V) = P_{\text{load}} \geq 0$, and let $P_{\text{crit}} = V_0^2/4r$. If $P_{\text{load}}/P_{\text{crit}} \leq 1$, then a simple calculation shows that (1) has solutions

$$V = \frac{V_0}{2}\left(1 \pm \sqrt{1 - \frac{P_{\text{load}}}{P_{\text{crit}}}}\right)\,,$$

Figure 4(b) plots these solutions as a function of P_{load}; depending on the ratio $P_{\text{load}}/P_{\text{crit}}$, the circuit can have two, one, or zero real-valued solutions. This example illustrates that even the existence of solutions depends heavily on the chosen load model. In Section VI-A we will revisit this feasibility problem for networks, and we will see that the maximum transfer limit P_{crit} generalizes as a Laplacian-like matrix encoding the topology and weights of the circuit graph.

D. Series circuit contraction and star-triangle transformation

Classic methods in the study of electric circuits are the contraction of a series of resistive circuit elements and the Y-Δ transformation; these methods date back to the work by Arthur E. Kennelly [86] and are depicted in Figures 5 and 6.

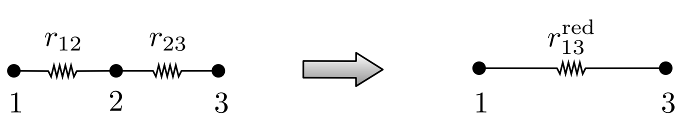

Fig. 5. Contraction of a series of resistive circuit elements to a single resistor.

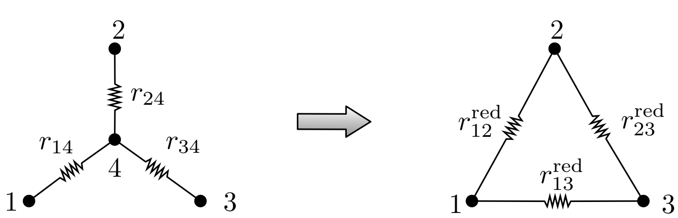

Fig. 6. Y-Δ transformation of a resistive radial circuit to a meshed circuit.

The reduced circuits are *equivalent* in their electrical behavior as seen from the terminals $\{1, 3\}$ (respectively, $\{1, 2, 3\}$) of the remaining nodes in the reduced single-resistor (respectively, three-node mesh) circuit. The well-known formula for the remaining single resistor in Figure 5 is

$$r_{13}^{\text{red}} = r_{12} + r_{23}\,,$$

and the formulas for the three-node mesh in Figure 6 are

$$\begin{aligned} r_{23}^{\text{red}} &= \frac{r_{14}r_{34} + r_{34}r_{24} + r_{24}r_{14}}{r_{14}}\,,\\ r_{12}^{\text{red}} &= \frac{r_{14}r_{34} + r_{34}r_{24} + r_{24}r_{14}}{r_{34}}\,,\\ r_{13}^{\text{red}} &= \frac{r_{14}r_{34} + r_{34}r_{24} + r_{24}r_{14}}{r_{24}}\,. \end{aligned} \tag{2}$$

At first glance, the circuit reduction formulae (2) appear convoluted and provide little immediate insight. In Section V however, we will show how these formulae can be insightfully derived by means of linear algebra and intuitively interpreted in terms of graph theory. Indeed, the series-circuit contraction and Y-Δ transformation are special cases of the more general *Kron reduction* [89] that permits an elegant analysis via algebraic graph theory.

III. Relevant Results in Algebraic Graph Theory

This section provides a concise self-contained review of algebraic graph theory, Perron-Frobenius theory, and their applications to row-stochastic and Laplacian matrices. We refer interested readers to the textbooks [16], [19], [72], [99] and, for example, the surveys [102], [97], [17]; this section follows the treatment in [27].

1) Notation: We briefly introduce the notation used in the remainder of the paper. For a vector $x \in \mathbb{R}^n$, the notation $\text{diag}(x)$ denotes a diagonal matrix in $\mathbb{R}^{n\times n}$ with the ith diagonal element being x_i, the average of its entries is denoted by $\text{average}(x) = \sum_{i=1}^n x_i/n$, and the extremum entries are $x_{\text{max}} = \max_{i\in\{1,\dots,n\}}\{x_i\}$ and $x_{\text{min}} = \min_{i\in\{1,\dots,n\}}\{x_i\}$.

We denote the real part (respectively, imaginary part) of a complex number $z \in \mathbb{C}$ by $\Re(z)$ (respectively, by $\Im(z)$).

The vector $\mathbb{e}_i$ denotes the ith canonical basis vector (with a non-zero and unit-entry at position i) in appropriate dimension. The symbols $\mathbb{0}_{n\times m}$ and $\mathbb{1}_{n\times m}$ denote the $(n \times m)$-matrices of all zero and unit entries. We avoid the subscript m in the vector-valued case $m = 1$ and entirely avoid subscripts when the dimension is clear from the content. The matrix $\Pi_n = I_n - \frac{1}{n}\mathbb{1}_{n\times n}$ denotes the orthogonal projection operator onto the subspace $\mathbb{1}_n^\perp = \{x \in \mathbb{R}^n \mid \mathbb{1}_n^\mathsf{T} x = 0\}$.

Element-wise (Hadamard) multiplication and division of matrices are denoted by $\odot$ and $\oslash$.

2) Nonnegative matrices and digraphs: Given $n \geq 2$, an $n \times n$ matrix A is nonnegative (resp. positive) if each entry is nonnegative (resp. positive); we write $A \geq 0$ and $A > 0$, respectively. A *weighted digraph* $\mathcal{G}$ is a triplet $(\{1, \dots, n\}, \mathcal{E}, A)$, where $\{1, \dots, n\}$ is a set of nodes, $\mathcal{E}$ is a set of directed edges (i.e., ordered pairs of nodes), and A is a weighted adjacency matrix (i.e., a nonnegative matrix) with the property that $a_{ij} > 0$ if and only if $(i, j) \in \mathcal{E}$. If $(i, j) \in \mathcal{E}$, we say i is the source and j is the sink of the directed edge. Given a nonnegative A, the weighted digraph *associated to* A has node set $\{1, \dots, n\}$ and edges defined by the patterns of non-zero entries of A. An *undirected graph* has undirected edges (i.e., the set $\mathcal{E}$ consists of unordered pairs of the form $\{i, j\}$) and a symmetric adjacency matrix $A = A^\mathsf{T}$.

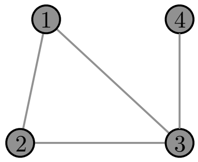

$$A = \begin{bmatrix} 0 & 1 & 1 & 0 \\ 1 & 0 & 1 & 0 \\ 1 & 1 & 0 & 1 \\ 0 & 0 & 1 & 0 \end{bmatrix}.$$

Fig. 7. An unweighted undirected graph and its adjacency matrix.

A *directed path* (resp. path) in a digraph (resp. graph) is an ordered sequence of nodes such that any pair of consecutive nodes in the sequence is a directed edge (resp. an undirected edge). A *simple* directed path (resp. path) is one with no repeated nodes, except possibly the first and last nodes. A *cycle* in an undirected graph is a simple path that starts and ends at the same vertex and has at least three distinct vertices. A *directed cycle* in a directed graph is a directed path that starts and ends at the same vertex. For the example in Figure 7, the sequence $(4, 3, 1, 3)$ is a path, $(1, 2, 3, 4)$ is a simple path, and $(1, 2, 3, 1)$ is a cycle.

3) Matrix irreducibility and digraph connectivity: A digraph (resp. graph) is *strongly connected* (resp. *connected*) if there exists a directed path (resp. path) from any node to any other node. A subgraph is a *strongly connected component* of a digraph $\mathcal{G}$ if it is strongly connected and no other node can be added to it while maintaing the subgraph strongly connected.

A nonnegative matrix A is *irreducible* if $\sum_{k=0}^{n-1} A^k > 0$ and *primitive* if there exists a number k such that $A^k > 0$. The matrix $A \geq 0$ is irreducible if and only if its associated digraph is strongly connected. The matrix $A \geq 0$ is primitive if and only if its associated digraph is strongly connected and *aperiodic*, i.e., there exists no natural number (except one) dividing the length of all directed cycles in $\mathcal{G}$. Clearly, if A is primitive, then it is irreducible; the converse is not true. For the example in Figure 7, one can see that A is irreducible because $A + A^2 > 0$, that A is primitive because $A^4 > 0$, and that the digraph associated to A (whereby each undirected edge is regarded as two directed edges) is strongly connected and aperiodic.

4) Perron-Frobenius theory for nonnegative matrices: The Perron-Frobenius Theorem states that, for any $A \geq 0$,

(i) there exist a real eigenvalue $\lambda \geq |\mu|$ for all other eigenvalues μ, and right and left nonnegative eigenvectors v_{right} and v_{left},
(ii) if A is irreducible, λ is positive and simple and v_{right} and v_{left} are unique and positive,
(iii) if A is primitive, $\lambda > |\mu|$ for all other eigenvalues μ.

Proofs of these statements are given for example in [99, Chapter 8]. The eigenvalue λ is called the *dominant eigenvalue* of A and, for irreducible matrices, its eigenvector (unique up to scaling) is called the *dominant eigenvector*.

The *spectral radius* of a square matrix A, denoted by $\rho(A)$, is the largest magnitude of its eigenvalues. The dominant eigenvalue of a nonnegative matrix is also its spectral radius. A known spectral bound is $\min_i (A\mathbb{1}_n)_i \leq \rho(A) \leq \max_i (A\mathbb{1}_n)_i$. For the example in Figure 7, one can see that the dominant eigenvaue $\lambda \approx 2.17$ lies in the interval $[1, 3]$.

5) Row-stochastic matrices: A matrix $A \geq 0$ is *row-stochastic* (resp. *column-stochastic*) if $A\mathbb{1}_n = \mathbb{1}_n$ (resp. $A^\mathsf{T}\mathbb{1}_n = \mathbb{1}_n$). The spectral bound implies that $\rho(A) = 1$ for any row-stochastic A. Clearly, the right dominant eigenvector of a row-stochastic matrix A is $\mathbb{1}_n$. A square matrix A is *semi-convergent* if $\lim_{k\to\infty} A^k$ is finite. If A is row-stochastic and primitive, then it is also semi-convergent and $\lim_{k\to\infty} A^k = \mathbb{1}_n v_{\text{left}}^\mathsf{T}$. More generally, a row-stochastic matrix A is semi-convergent if and only if each strongly connected component of $\mathcal{G}$ without out-going edges is aperiodic. Proofs of these statements are given for example in [27, Chapters 4 and 5].

6) Laplacian matrices and their algebraic connectivity: A matrix $\mathcal{L} \in \mathbb{R}^{n\times n}$ is *Laplacian* if $\mathcal{L}\mathbb{1}_n = \mathbb{0}_n$ and its off-diagonal entries are nonpositive. The Laplacian matrix of a weighted digraph is defined by $\mathcal{L} = \operatorname{diag}(A\mathbb{1}_n) - A$; vice versa, the weighted digraph $\mathcal{G}$ *associated to* a Laplacian matrix $\mathcal{L}$ is defined by setting $a_{ij} = -\ell_{ij}$ for $i \neq j$. $\mathcal{L}$ is said to be irreducible if $\mathcal{G}$ is strongly connected. Laplacian matrices have remarkable properties. The matrix $\mathcal{L}$ is singular and all its eigenvalues different from zero have positive real part. The matrix $\mathcal{L}$ is irreducible if and only if the rank of $\mathcal{L}$ is $n-1$; in this case $\operatorname{Im}(\mathcal{L}) = \mathbb{1}_n^\perp$. If $\mathcal{L}$ is symmetric (or equivalently, $\mathcal{G}$ is undirected), then the eigenvalues of $\mathcal{L}$ can be ordered as $0 = \lambda_1 \leq \lambda_2 \leq \cdots \leq \lambda_n$ and $\mathcal{G}$ is connected if and only if $\lambda_2 > 0$. The smallest non-zero eigenvalue λ_2 is called the *algebraic connectivity* of $\mathcal{G}$. Finally, let $\exp$ denote the matrix exponential operation; if $\mathcal{G}$ contains a globally reachable node, then $\lim_{t\to+\infty} \exp(-\mathcal{L}t) = \mathbb{1}_n v_{\text{left}}^\mathsf{T}$, where v_{left} denotes the nonnegative left eigenvector of $\mathcal{L}$ with eigenvalue 0, normalized to satisfy $\mathbb{1}_n^\mathsf{T} v_{\text{left}} = 1$. The rate of convergence of $\exp(-\mathcal{L}t)$ is determined by the algebraic connectivity λ_2. Proofs of these statements are given for example in [27, Chapters 6 and 7].

7) Metzler matrices and their properties: A matrix M is *Metzler* if its off-diagonal entries are nonnegative. If $\mathcal{L}$ is Laplacian, $-\mathcal{L}$ is Metzler. The weighted digraph $\mathcal{G}$ associated to M is defined by $a_{ij} = m_{ij}$ for $i \neq j$. The Perron-Frobenius Theorem for Metzler matrices states that, for any Metzler matrix M,

(i) there exist a real eigenvalue $\lambda \geq \Re(\mu)$ for all other eigenvalues μ, and right and left nonnegative eigenvectors v_{right} and v_{left},
(ii) if M is irreducible, λ is simple and v_{right} and v_{left} are unique and positive.

A Metzler matrix is Hurwitz if its dominant eigenvalue (and therefore all its eigenvalues) has negative real part. A Metzler matrix M is Hurwitz if and only if M is invertible and $-M^{-1}$ is nonnegative. Moreover, if M is Metzler, Hurwitz, and irreducible, then $-M^{-1}$ is a strictly positive matrix. One can show that (i) any Metzler matrix M can be written as $M_0 + \operatorname{diag}(v)$, where M_0 has zero row-sums (or alternatively column-sums) and $v \in \mathbb{R}^n$, and that (ii) if v has non-positive entries and at least one entry strictly negative, then the Metzler matrix $M_0 + \operatorname{diag}(v)$ is Hurwitz. Proofs of these statements are given for example in [27, Chapter 9].

Metzler matrices and their algebraic and graph-theoretical properties are the central objects in the study of linear compartmental systems, an instance of which are circuits. We refer to Appendix A for a self-contained treatment.

8) Incidence matrices and their properties: Given an undirected graph $\mathcal{G}$ with n nodes and m edges, assign to each edge of $\mathcal{G}$ a unique index $e \in \{1, \dots, m\}$ and an arbitrary direction. The *(oriented) incidence matrix* $B \in \mathbb{R}^{n\times m}$ of $\mathcal{G}$ is defined by

$$B_{ie} = \begin{cases} +1, & \text{if the edge } e \text{ is } (i,j) \text{ for some } j, \\ -1, & \text{if the edge } e \text{ is } (j,i) \text{ for some } j, \\ 0, & \text{otherwise.} \end{cases}$$

Clearly, $\mathbb{1}_n^\top B = \mathbb{0}_m^\top$. Moreover, if $\operatorname{diag}(\{a_e\}_{e\in\{1,\dots,m\}})$ is the diagonal matrix of edge weights, then the Laplacian of $\mathcal{G}$ satisfies $\mathcal{L} = B \operatorname{diag}(\{a_e\}_{e\in\{1,\dots,m\}}) B^\top$. The undirected graph $\mathcal{G}$ is connected if and only if the rank of B is $n-1$.

We next consider an illustrative example in the next figure.

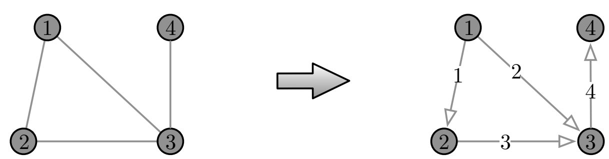

Fig. 8. Numbering and orienting the edges of an undirected graph.

For the undirected unweighted graph on the left (and its oriented version on the right), the incidence matrix B and the Laplacian matrix $\mathcal{L}$ are, respectively,

$$B = \begin{bmatrix} +1 & +1 & 0 & 0 \\ -1 & 0 & +1 & 0 \\ 0 & -1 & -1 & +1 \\ 0 & 0 & 0 & -1 \end{bmatrix}, \quad \mathcal{L} = \begin{bmatrix} 2 & -1 & -1 & 0 \\ -1 & 2 & -1 & 0 \\ -1 & -1 & 3 & -1 \\ 0 & 0 & -1 & 1 \end{bmatrix}.$$

As one can verify, $\mathbb{1}_n^\top B = \mathbb{0}_m^\top$ and $\mathcal{L}$ is positive semidefinite.

9) Cycle and cutset spaces: Let $\mathcal{G}$ be an undirected unweighted graph with node set $\{1, \dots, n\}$ and m edges. Number the edges of $\mathcal{G}$ with a unique identifier $e \in \{1, \dots, m\}$ and assign an arbitrary direction to each edge.

A *cut* χ of $\mathcal{G}$ is a strict non-empty subset of nodes. A cut and its complement χ^{c} define a partition $\{1, \dots, n\} = \chi \cup \chi^{\mathsf{c}}$. Given a cut χ, the set of edges that have one endpoint in each subset of the partition is called the *cutset* of χ.

Given a simple undirected path γ in $\mathcal{G}$, the *signed path vector* $v^\gamma \in \{-1, 0, +1\}^m$ of γ is defined by, for $e \in \{1, \dots, m\}$,

$$v_e^\gamma = \begin{cases} +1, & \text{if } e \text{ is traversed positively by } \gamma, \\ -1, & \text{if } e \text{ is traversed negatively by } \gamma, \\ 0, & \text{otherwise.} \end{cases}$$

Given a cut χ of $\mathcal{G}$, the *cutset orientation vector* $v^\chi \in \{-1, 0, +1\}^m$ of the cut has components

$$v_e^\chi = \begin{cases} +1, & \text{if } e \text{ has its source in } \chi \text{ and sink in } \chi^{\mathsf{c}}, \\ -1, & \text{if } e \text{ has its sink in } \chi \text{ and source in } \chi^{\mathsf{c}}, \\ 0, & \text{otherwise.} \end{cases}$$

Here the source (resp. sink) of a directed edge (i,j) is the node i (resp j). Figure 9 illustrates these notions.

The *cycle space* of $\mathcal{G}$ is the subspace of $\mathbb{R}^m$ spanned by the signed path vectors corresponding to all simple undirected cycles in $\mathcal{G}$, that is, $\operatorname{span}\{v^\gamma \in \mathbb{R}^m \mid \gamma \text{ is a simple cycle in } \mathcal{G}\}$.

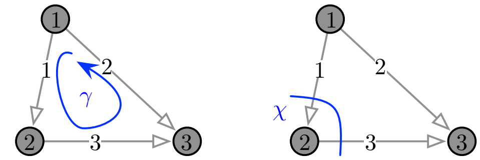

Fig. 9. A simple cycle γ and a cut χ with corresponding signed path vector $v^\gamma = [+1 \ \ -1 \ \ +1]^\top$ and cutset orientation vector $v^\chi = [-1 \ \ 0 \ \ +1]^\top$.

The *cutset space* of $\mathcal{G}$ is subspace of $\mathbb{R}^m$ spanned by the cutset orientation vectors corresponding to all cuts of the nodes of $\mathcal{G}$, that is, $\operatorname{span}\{v^\chi \in \mathbb{R}^m \mid \chi \text{ is a cut of } \mathcal{G}\}$. The following linear algebraic statements follow [27, Chapter 8] easily:

(S1) the cycle space is $\operatorname{Ker}(B)$,
(S2) the cutset space is $\operatorname{Im}(B^\top)$, and
(S3) $\operatorname{Ker}(B) \perp \operatorname{Im}(B^\top)$ and $\operatorname{Ker}(B) \oplus \operatorname{Im}(B^\top) = \mathbb{R}^m$.

Statement (S3) is also known as a statement in the fundamental theorem of linear algebra.

IV. General models of electrical networks

In the following, we develop a rather general electrical network model and connect it to the algebraic graph theory concepts introduced in Section III. We will use the language of graph theory, but we remark that many alternative terminologies arose in different disciplines of electrical engineering (circuits, electronics, power, etc.). For example, graph-theoretic concepts such as nodes and edges are often referred to as buses, terminals, branches, lines, and so on. Likewise, all of the aforementioned graph matrices can be found under multiple different names and sign-conventions, but we will consistently use the terminology from Section III.

A. Electrical network modeling

1) Topology and variables: An electrical network is an undirected graph $\mathcal{G} = \{\{1, \dots, n\}, \mathcal{E}\}$ composed of n nodes and m undirected edges $\mathcal{E}$. Additionally, we introduce a separate *ground node* $\{0\}$ denoting the common electrical ground and a separate edge set $\mathcal{E}_0 = \cup_{i\in\{1,\dots,n\}}\{i, 0\}$ connecting each node $i \in \{1, \dots, n\}$ to the ground. Without loss of generality, we select an arbitrary orientation for each undirected edge $\{i,j\} \in \mathcal{E} \cup \mathcal{E}_0$ and, specifically, orient all edges of the form $\{i, 0\}$ as $(i, 0)$. For each directed edge (i,j) we define

- an oriented *current flow* $f_{ij} \in \mathbb{R}$, and
- an oriented *voltage drop* $u_{ij} \in \mathbb{R}$.

As in Section III-8, the topology of the oriented edges among the nodes $\{1, \dots, n\}$ (excluding the ground node) is encoded by the oriented incidence matrix B of $\mathcal{G}$. When including the ground node $\{0\}$ and its associated edges, the overall incidence matrix takes the form

$$B_{\text{ground}} = \left[\begin{array}{c|c} -\mathbb{1}_n^\top & \mathbb{0}_m^\top \\ \hline I_n & B \end{array}\right] \in \mathbb{R}^{(1+n)\times(n+m)}.$$

We remark that the choice of edge numbering and orientation is arbitrary; the latter simply reflects the reference directions for the variables u_{ij} and f_{ij}. We will later also use the vectors u and f that collect the variables u_{ij} and f_{ji}, for $\{i,j\} \in \mathcal{E}$, with elements ordered in correspondence with the numbering of the edges. Next we introduce Kirchhoff's laws and reveal the role of the ground node $\{0\}$.

2) Kirchhoff's laws: In our graph-theoretic setting we take Kirchhoff laws as two fundamental axioms that define the fundamental physics of electrical networks [87]:

- *Kirchhoff's current law* (KCL): For each node in the network, the algebraic sum of all current flows incident to the node must be zero. Specifically, for all nodes $i \in \{0\} \cup \{1, \dots, n\}$, the current flow balance is:
$$0 = \sum_{j \text{ s.t. } (i,j) \in \mathcal{E} \cup \mathcal{E}_0} f_{ij} - \sum_{j \text{ s.t. } (j,i) \in \mathcal{E} \cup \mathcal{E}_0} f_{ji} \,,$$
where, slightly abusing notation, $(i,j) \in \mathcal{E} \cup \mathcal{E}_0$ denotes the oriented edge $\{i,j\}$ taken from the original set of non-oriented edges $\mathcal{E} \cup \mathcal{E}_0$. More generally, for any graph cut χ with cutset orientation vector v^χ,
$$0 = \sum_{e \in \mathcal{E} \cup \mathcal{E}_0} v_e^\chi f_e, \tag{3}$$
These equations can be rewritten compactly as follows. Equation (3) implies that the vector of current flows $f \in \mathbb{R}^m$ is perpendicular to the cutset orientation vector v^χ of every cut and, thus, to the subspace $\mathrm{Im}(B_{\text{ground}}^\mathsf{T})$. Statements (S1) and (S3) in Section III-9 imply that $f \in \mathrm{Ker}(B_{\text{ground}})$ so that
$$\mathbb{0}_{n+1} = B_{\text{ground}} \begin{bmatrix} f_0 \\ f \end{bmatrix} \,, \tag{4}$$
where $f_0 \in \mathbb{R}^n$ is the vector of components f_{i0}.
- *Kirchhoff's voltage law* (KVL): For all simple undirected cycles in the network, the algebraic sum of all directed voltage drops along the (oriented) edges of the cycle must be zero. Specifically, for each simple undirected cycle γ with signed path vector v^γ, the voltage drop sum is:
$$0 = \sum_{(i,j) \in \gamma} v_{(i,j)}^\gamma u_{ij} \,, \tag{5}$$
These equations can be rewritten as follows. Equality (5) implies that the vector of voltage drops $u \in \mathbb{R}^m$ is perpendicular to the signed path vector v^γ of every cycle and, thus, to the subspace $\mathrm{Ker}(B_{\text{ground}})$. Statements (S2) and (S3) in Section III-9 imply that $u \in \mathrm{Im}(B_{\text{ground}}^\mathsf{T})$ and, thus, that there exist so-called *potential* variables $V_0 \in \mathbb{R}$ and $V \in \mathbb{R}^n$ such that
$$\begin{bmatrix} u_0 \\ u \end{bmatrix} = B_{\text{ground}}^\mathsf{T} \begin{bmatrix} V_0 \\ V \end{bmatrix} \,, \tag{6}$$
where $u_0 \in \mathbb{R}^n$ is the vector of components u_{i0}.

Note that the fundamental theorem of linear algebra, as presented in statement (S3) in Section III-9, together with equations (4) and (6), imply that
$$\begin{bmatrix} f_0 \\ f \end{bmatrix}^\mathsf{T} \begin{bmatrix} u_0 \\ u \end{bmatrix} = 0 \,,$$
that is, the sum of all instantaneous *power flows* $f_{ij} \cdot u_{ij}$ along all edges $\{i,j\}$ in the network equals zero. This general fact, direct consequence of the properties of cutset and cycle spaces in Section III-9, is known as *Tellegen's Theorem* [127] in network analysis. Tellegen's Theorem is extremely general and holds independently of the (linear or possibly nonlinear) dynamic and static characteristics of an electrical network.

3) The ground node: It is convenient to specify for each node $i \in \{1, \dots, n\}$ two separate variables denoting its current flow and voltage with respect to the ground. We define*

- the current flow $I_i = -f_{i0} \in \mathbb{R}$ from the ground to each node $i \in \{1, \dots, n\}$ in KCL (4) as the *external current injection*; and
- a *potential* $V_i \in \mathbb{R}$ as an auxiliary variable for each node $i \in \{1, \dots, n\} \cup \{0\}$ to specify KVL (6).

Observe that KVL (6) defines the potentials V_i only up to an arbitrary reference since $\mathbb{1}_{n+1} \in \mathrm{Ker}(B_{\text{ground}}^\mathsf{T})$. It is convenient to define the potential of the electrical ground as zero:

- *ground potential*: the ground has zero potential: $V_0 = 0$.

We can now write Kirchhoff's laws in a way that is more familiar to scholars of graph theory [17] and dynamical systems [135]. KCL (4) reads for nodes $\{1, \dots, n\}$ as
$$I = Bf \,. \tag{7}$$
For the ground $\{0\}$, KCL gives the current injection balance
$$\sum\nolimits_{i=1}^n I_i = 0 \,. \tag{8}$$
Observe that this balance equation is redundant as it can also be found by multiplying KCL (7) from the left by $\mathbb{1}_n^\mathsf{T}$.

Given that $V_0 = 0$, KVL (6) gives the voltage u_{i0} between node i and the ground $\{0\}$ simply as the potential V_i:
$$u_{i0} = V_i \,, \quad \text{for all } i \in \{1, \dots, n\} \,.$$
Let $u \in \mathbb{R}^m$ be the vector that collects all other voltages u_{ij} for $\{i,j\} \in \mathcal{E}$ with appropriate numbering. Then KVL (6) can be written as
$$u = B^\mathsf{T} V \,, \tag{9}$$
that is, the voltage drops equal potential differences $u_{ij} = V_i - V_j$ for each $\{i,j\} \in \mathcal{E}$ with the sign convention as specified by the oriented incidence matrix B.

Kirchhoff's laws (7), (9) define $n+m$ linear equations relating the $2n+2m$ variables (V, I, f, u). We further complement these equations through constitutive relations relating f_{ij} and u_{ij} for any pair $\{i,j\}$ of connected nodes.

4) Constitutive relations: Here we consider three basic linear circuit elements: resistors, inductors, and capacitors. These three elements are illustrated with their circuit symbols in Figure 10. The voltage u_{ij} over a circuit element and current flow f_{ij} through it satisfy the following well-known constitutive relations:

- resistor: $u_{ij} = r_{ij} f_{ij}$, where $r_{ij} > 0$ is a resistance;
- inductor: $\ell_{ij} \frac{\mathrm{d}}{\mathrm{d}t} f_{ij} = u_{ij}$, where $\ell_{ij} > 0$ is an inductance;
- capacitor: $c_{ij} \frac{\mathrm{d}}{\mathrm{d}t} u_{ij} = f_{ij}$, where $c_{ij} > 0$ is a capacitance.

The constitutive relation for a resistor, $u_{ij} = r_{ij} f_{ij}$ known as *Ohm's law* gives together with KVL (9) the current flow over the resistor as $f_{ij} = u_{ij}/r_{ij} = (V_i - V_j)/r_{ij}$. It is instructive

*Our notation follows the convention that nodal (respectively, edge) variables are denoted by capital (respectively, lower-case) letters.

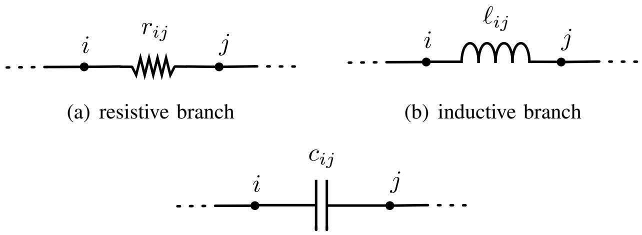

(a) resistive branch (b) inductive branch

(c) capacitive branch

Fig. 10. Circuit symbols for resistors, inductors, and capacitors

to remark that this flow function $f_{ij} = (V_i - V_j)/r_{ij}$ can also be derived as the unique flow-characteristic that minimizes the network losses subject to KCL (7) and assuming anti-symmetry $f_{ij} = -f_{ji}$ of the flow. This result, known as *Thomson's Principle*, is nowadays an integral part of textbooks on algebraic graph theory and Markov chains [77], [55], [61].

We will collectively refer to resistors, inductors, and capacitors as *impedances*, a term which is also often used when multiple basic circuit elements are lumped into a single one.

5) Load models: For the ground $\{0\}$ we omit the double-indexing of adjacent circuit elements, and use c_i, l_i, and r_i instead of c_{i0}, l_{i0}, and r_{i0}. Circuit elements (or a collection thereof) connected to the ground are referred to as *shunt impedances*, and they are often used to model loads. In particular, a shunt resistor r_i injects a load current $I_{\text{load},i} = -f_{i0} = -u_{i0}/r_i = -V_i/r_i$ and models so-called *active power loads* which dissipate energy. On the contrary shunt capacitors and inductors model so-called *reactive power loads* that merely transform energy; see Section VI-B. Aside from such *impedance loads*, which draw a current $I_{\text{load},i}$ linearly depending on the potential V_i, another popular load model is a *constant current demand* $I_{\text{load},i} = I_i^* \in \mathbb{R}_{\leq 0}$ or more general nonlinear relations between load current $I_{\text{load},i}$ and the potential V_i, e.g., a load injecting a constant instantaneous power $P_i^* = I_{\text{load},i}\, V_i \leq 0$. A load model aggregating constant impedance, constant current, and constant power loads is normally called a ZIP load [90]. We refer to Figure 11 for an illustration of such load models.

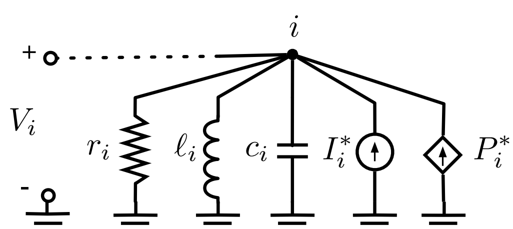

Fig. 11. A load model aggregating a shunt impedance (r_i, l_i, c_i), a constant current load I_i^*, and a constant power load with constant $P_i^* = I_{\text{load},i} V_i$.

6) Source models: A device that provides a constant current injection $I_i = I_i^* \in \mathbb{R}_{\geq 0}$ or a constant potential $V_i^* \in \mathbb{R}_{\geq 0}$ (relative to the ground) at a node i is termed an *ideal current source* or an *ideal voltage source*, respectively. Figure 12 depicts an ideal current source and voltage source in combination with a shunt resistor r_i and with a series resistance r_{ik}, respectively. We show these resistances for the following reason: When we set $r_i = r_{ki}$ and $V_k^*/r_{ki} = I_i^*$, then by Ohm's law these two models are delivering the same current

$$I_i = I_i^* - V_i/r_i = (V_k^* - V_i)/r_{ki}.$$

Thus, an ideal voltage source can always be converted to an ideal current source and vice versa. In the following, we focus without loss of generality on constant current sources.

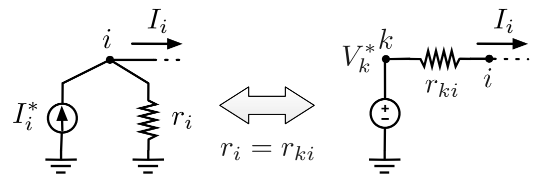

Fig. 12. Equivalent constant current and constant voltage sources

B. Different branch models

Kirchhoff's laws, the constitutive relations, and the models for loads and sources provide the required ingredients for our network model. We connect the loads and sources through a network whose branches are modeled by lumped circuit elements taking into account losses, charging, waves, and other effects. A widely used branch model is the Π-model depicted in Figure 13. The Π-model consists of a series resistive-inductive impedance modeling the branch inductance and losses as well as a shunt capacitor to ground at each end of the branch modeling the cable charging. Typically, the two shunt capacitors take identical values.

The Π-model can be used to model various branch characteristics, including long high-voltage transmission lines (dominantly inductive), underground cables (with additional resistive and capacitive components), and short wires (dominantly resistive) [90], [106]. Note that if there are multiple branches connected to a node, each modeled by the Π-model, we can merge the multiple parallel shunt capacitors into a single one.

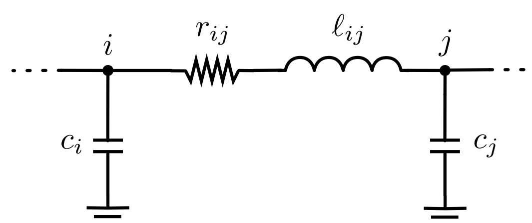

Fig. 13. Π-model of a branch in electrical network between nodes i and j.

C. A prototypical electrical network

In what follows, we consider a prototypical electrical network model to illustrate applications of algebraic graph theory. For each branch we consider a Π-model as in Figure 13. When multiple Π-models are connected to the same node, we lump all parallel capacitors into a single equivalent capacitance. At each node $i \in \{1, \dots, n\}$ we thus consider an equivalent capacitance $c_i > 0$, a shunt resistance $r_i \geq 0$, a constant current injection $I_i^* \in \mathbb{R}$, and a constant power injection $P_i^* \in \mathbb{R}$ modeling sources and loads as in Figures 11 and 12. In this case, the network equations are

$$\begin{aligned} &\text{KCL:} && I = Bf\,, && \text{(10a)}\\ &\text{KVL:} && u = B^\mathsf{T} V\,, && \text{(10b)}\\ &\text{ground:} && I = I_{\text{load}} - C\dot{V}\,, && \text{(10c)}\\ &\text{branch:} && L\dot{f} = u - Rf\,, && \text{(10d)}\\ &\text{load:} && I_{\text{load}} = I^* + P^* \oslash V - GV\,, && \text{(10e)} \end{aligned}$$

where R, L, C, G are diagonal matrices of r_{ij}, ℓ_{ij}, c_i, and the symbol $g_i = 1/r_i$ conventionally denotes the shunt conductance (reciprocal of resistance). Finally, $I^* = (I_1^*, \ldots, I_n^*)$ and P^* are the vectors of constant current and power injections.

It is convenient to reduce the network equations (10) to a state-space model defined in terms of the variables V and f associated with the capacitive and inductive storage elements. By inserting (10a), (10e) in (10c), respectively, (10b) in (10d), we obtain

$$\begin{bmatrix} C & \\ & L \end{bmatrix} \begin{bmatrix} \dot{V} \\ \dot{f} \end{bmatrix} = \begin{bmatrix} -G & -B \\ B^\mathsf{T} & -R \end{bmatrix} \begin{bmatrix} V \\ f \end{bmatrix} + \begin{bmatrix} I^* + P^* \oslash V \\ \mathbb{0}_m \end{bmatrix}. \quad (11)$$

A block-diagram of the electrical network model (10), respectively, (11), is shown in Figure 14. Observe the separation of the dynamics associated to n nodes (ground and loads) and m edges (branches), the exogenous current injections I^* and nonlinear power injections P^*, as well as the interconnection through Kirchhoff's current and voltage laws via B and $B^\top$.

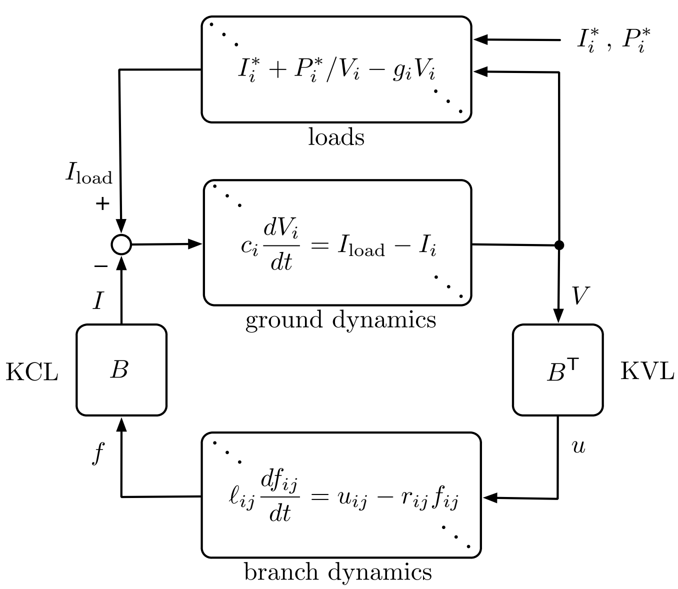

Fig. 14. Block-diagram of the electrical network model (10).

D. Noteworthy special cases

The electrical network model described in equations (10) and (11), respectively, is fairly general and admits a few special cases that we will repeatedly revisit as pedagogical examples.

1) Resistive-capacitive interconnection: If all branches are purely resistive (R positive definite and $L = \mathbb{0}_{m\times m}$), the model (11) reduces to

$$C\dot{V} = -\left(\mathcal{L}_R + G\right)V + I^* + P^* \oslash V\,, \qquad (12)$$

where $\mathcal{L}_R = BR^{-1}B^\mathsf{T}$ is the so-called *conductance matrix*, a Laplacian matrix associated with the (undirected) graph of the electrical network with weights given by inverse resistance $1/r_{ij}$ for edge $\{i,j\}$; see Section III-8. We will later reveal various properties of the nonlinear dynamic equations (12) by studying the properties of the matrix $BR^{-1}B^\mathsf{T} + G$.

In the absence of constant-power loads ($P^* = \mathbb{0}_n$), equilibrium points of (12) are determined by a static and well-studied model characterized by the Laplacian matrix $\mathcal{L}_R$ and the conductance loads G:

$$I^* = (\mathcal{L}_R + G)V\,. \qquad (13)$$

2) Lossless inductive-capacitive case: In the absence of loads ($G = \mathbb{0}_{n\times n}$ and $I^* = P^* = \mathbb{0}_n$) and dissipative elements ($R = \mathbb{0}_{m\times m}$) — that is, in an entirely lossless circuit — the electrical network model (11) can be re-written as

$$\begin{bmatrix} C & \\ & L \end{bmatrix} \begin{bmatrix} \dot{V} \\ \dot{f} \end{bmatrix} = \begin{bmatrix} \mathbb{0} & -B \\ B^\mathsf{T} & \mathbb{0} \end{bmatrix} \begin{bmatrix} V \\ f \end{bmatrix}, \qquad (14)$$

or by taking another derivative of V, as

$$C\ddot{V} = -\mathcal{L}_L V\,, \qquad (15)$$

where $\mathcal{L}_L = BL^{-1}B^\mathsf{T}$ is the weighted Laplacian matrix with weights L^{-1}.

3) Homogeneous case: Consider a slightly more complex scenario, where all network branches are made of the same material, and thus the ratio of $l_{ij}/r_{ij} = \tau$ is constant for all edges $\{i,j\} \in \mathcal{E}$. Assume also that there are no constant-current or constant-power loads, so that $I^* = P^* = \mathbb{0}_n$. By taking a second derivative of V in (11), substituting for $\dot{f}$, and finally eliminating f, the electrical network model (11) can be re-written as

$$\tau C\ddot{V} + (\tau G + C)\dot{V} + (\mathcal{L}_R + G)V = \mathbb{0}_n\,. \qquad (16)$$

For $\tau = 0$, we recover the model (12) and for $\tau = \infty$ and $G = \mathbb{0}_{n\times n}$, we recover the model (15). The equations (16) are also reminiscent of the resistively coupled LC tanks introduced in Section II-A. The LC tanks can be modeled by the equations

$$C\ddot{V} + \mathcal{L}_R\dot{V} + L^{-1}V = \mathbb{0}_n\,, \qquad (17)$$

where V is the vector of voltages across every LC tank circuit [49]. In the homogeneous case in Section II-A, i.e., for $R = rI_m$, $C = cI_n$, and $L = \ell I_n$, the model (17) reduces to

$$\ddot{V} + \tau'\mathcal{L}\dot{V} + \omega_0^2 V = \mathbb{0}_n\,,$$

where we recall that $\omega_0 = 1/\sqrt{\ell c}$ is the natural frequency of oscillations, $\mathcal{L} = BB^\mathsf{T}$ is the unweighted Laplacian of the network, and $\tau' = 1/rc$ is a uniform time-constant that determines the relaxation time to the synchronous solution.

In the following sections, we analyze the static and dynamic properties of the electrical network model (10) and its special cases from the viewpoint of algebraic graph theory. We remark that most of the following approaches extend (either directly or at least conceptually) to richer classes of electrical networks with switching behavior as in power electronics [60], [162], multi-physical dynamics as in synchronous generators [63], [74], or nonlinear oscillators [152], [47], [39], among others.

V. Structure and Dynamics of Linear Electrical Networks

In what follows, we explain how the structure of an electrical network (in terms of its topology and impedances) reveals various insights about the associated electrical dynamics. The interplay of structure and dynamics is revealed through the algebraic graph theory methods introduced in Section III. This section focuses on the case of linear electrical networks, described by special cases of the general model (11). The study of nonlinear networks is deferred to Section VI.

A. Static resistive networks

We begin our analysis with the case of a static resistive network with no constant power loads, as described by (13). For simplicity of notation, let us drop the super- and subscripts in this section and simply rewrite (13) as

$$I = (\mathcal{L} + G)V\,, \tag{18}$$

where $\mathcal{L} = \mathcal{L}^\mathsf{T} \in \mathbb{R}^{n\times n}$ is a symmetric and irreducible Laplacian matrix, $G \in \mathbb{R}^{n\times n}$ is a diagonal matrix with nonnegative diagonal entries, and $I, V \in \mathbb{R}^n$ are constant vectors. We remark that equation (18) is also of interest independently of circuits, as linear diffusive equations with Laplacian matrices arise all throughout the sciences [138].

1) Characteristics of solutions and Laplacian inverses: We explore the solution space of the resistive circuit equation (18). We consider the singular and non-singular case separately.

Singular circuit equations: When $G = \mathbb{0}_{n\times n}$, we know from Section III-6 that $\mathcal{L}$ is singular with $\mathrm{Ker}(\mathcal{L}) = \mathrm{span}(\mathbb{1}_n)$ and with $\mathrm{Im}(\mathcal{L}) = \mathbb{1}_n^\perp$. Hence, equation (18) admits a solution if and only if $I \in \mathbb{1}_n^\perp$, that is, the current injections are balanced: $\mathbb{1}_n^\mathsf{T} I = 0$. In this case, the solution is given by

$$V = V_{\text{hom}} + V_{\text{part}} = \alpha \cdot \mathbb{1}_n + \mathcal{L}^\dagger I\,, \tag{19}$$

where the homogeneous solution $V_{\text{hom}} = \alpha \cdot \mathbb{1}_n$ with $\alpha \in \mathbb{R}$ is the *flat-voltage profile* without current flows, and the particular solution is $V_{\text{part}} = \mathcal{L}^\dagger I \in \mathbb{1}_n^\perp$, where $\mathcal{L}^\dagger$ is the Moore-Penrose inverse of the Laplacian matrix $\mathcal{L}$ [99]. The following proposition collects some properties of the various possible generalized inverses of a Laplacian matrix.

Proposition 5.1 (Inverse Laplacian matrices [27], [52], [75], [38], [69]): Consider a symmetric and irreducible Laplacian matrix $\mathcal{L} \in \mathbb{R}^{n\times n}$ with singular value decomposition

$$\mathcal{L} = \underbrace{\begin{bmatrix} \frac{1}{\sqrt{n}}\mathbb{1}_n & v_2 & \dots & v_n \end{bmatrix}}_{=\mathbb{V}} \begin{bmatrix} 0 & & & \\ & \lambda_2 & & \\ & & \ddots & \\ & & & \lambda_n \end{bmatrix} \underbrace{\begin{bmatrix} \frac{1}{\sqrt{n}}\mathbb{1}_n & v_2 & \dots & v_n \end{bmatrix}^\mathsf{T}}_{=\mathbb{V}^\mathsf{T}},$$

where $\lambda_2, \dots, \lambda_n > 0$ and $v_2, \dots, v_n \perp \mathbb{1}_n$ are the nonzero eigenvalues of $\mathcal{L}$ and associated eigenvectors collected in the matrix $\mathbb{V}$. The following statements hold:

(i) the Moore-Penrose inverse of $\mathcal{L}$ given by

$$\mathcal{L}^\dagger = \mathbb{V} \begin{bmatrix} 0 & & & \\ & \frac{1}{\lambda_2} & & \\ & & \ddots & \\ & & & \frac{1}{\lambda_n} \end{bmatrix} \mathbb{V}^\mathsf{T} \tag{20}$$

is symmetric positive semidefinite, with zero row and column sums, and satisfies $\mathcal{L}^\dagger \mathcal{L} = \mathcal{L}\mathcal{L}^\dagger = \Pi_n$;

(ii) the *regularized Laplacian* $\mathcal{L}_{\text{reg}} = \mathcal{L} + \frac{\beta}{n}\mathbb{1}_n\mathbb{1}_n^\mathsf{T}$ with $\beta > 0$ is non-singular, positive definite, and satisfies

$$\begin{aligned} \mathcal{L}_{\text{reg}}^{-1} &= \left(\mathcal{L} + \frac{\beta}{n}\mathbb{1}_n\mathbb{1}_n^\mathsf{T}\right)^{-1} = \mathcal{L}^\dagger + \frac{1}{\beta\, n}\mathbb{1}_n\mathbb{1}_n^\mathsf{T} \\ &= \mathbb{V} \begin{bmatrix} \frac{1}{\beta} & & & \\ & \frac{1}{\lambda_2} & & \\ & & \ddots & \\ & & & \frac{1}{\lambda_n} \end{bmatrix} \mathbb{V}^\mathsf{T}\,; \end{aligned} \tag{21}$$

(iii) the *shunted Laplacian* $\mathcal{L}_{\text{shunt}} = \mathcal{L} + \varepsilon I_n$ with $\varepsilon > 0$ is non-singular, positive definite, and satisfies

$$\mathcal{L}_{\text{shunt}}^{-1} = \mathbb{V} \begin{bmatrix} \frac{1}{\varepsilon} & & & \\ & \frac{1}{\lambda_2+\varepsilon} & & \\ & & \ddots & \\ & & & \frac{1}{\lambda_n+\varepsilon} \end{bmatrix} \mathbb{V}^\mathsf{T}\,; \tag{22}$$

(iv) the *grounded Laplacian* $\mathcal{L}_{\text{ground}} \in \mathbb{R}^{(n-1)\times(n-1)}$ is the leading principal $(n-1)\times(n-1)$ submatrix of the Laplacian matrix $\mathcal{L}$ (after removing the nth row and nth column) and has the following properties: $\mathcal{L}_{\text{ground}}$ is non-singular and positive definite, $-\mathcal{L}_{\text{ground}}$ is a Metzler matrix, and its inverse is a nonnegative matrix satisfying

$$\left(\mathcal{L}_{\text{ground}}^{-1}\right)_{ij} = (\mathbb{e}_i - \mathbb{e}_n)^\mathsf{T} \mathcal{L}^\dagger (\mathbb{e}_j - \mathbb{e}_n)\,. \tag{23}$$

The regularized Laplacian $\mathcal{L}_{\text{reg}}$, the shunted Laplacian $\mathcal{L}_{\text{shunt}}$, and the grounded Laplacian $\mathcal{L}_{\text{ground}}$ are all non-singular and positive definite matrices. Due to these favorable properties they are often preferred for numerical computations or for analytic studies, as compared to the singular Laplacian $\mathcal{L}$ that requires careful treatment of its nullspace. Note that the regularized and shunted Laplacians $\mathcal{L}_{\text{reg}}$ and $\mathcal{L}_{\text{shunt}}$ have the same eigenvectors as the Laplacian $\mathcal{L}$, but the zero (respectively, all) eigenvalues are shifted to the right. The inverse Laplacian matrices (20)-(22) are sometimes referred to as *Green matrices* and studied in different applications [21], [92], [61], [31]. On the other hand, the grounded Laplacian $\mathcal{L}_{\text{ground}}$ and its inverse do not preserve the eigenstructure of $\mathcal{L}$; see [109], [153] for relations between $\mathcal{L}$ and $\mathcal{L}_{\text{ground}}$.

Aside from mathematical convenience, the grounded Laplacian $\mathcal{L}_{\text{ground}}$ is also a natural concept in circuit analysis when the nth node is literally the ground of the circuit [37]. Vice versa, the matrix $\mathcal{L}_R + G$ in (13) can be thought of as the grounded Laplacian of a network with $n+1$ nodes. Along the same lines, the shunted Laplacian $\mathcal{L}_{\text{shunt}}$ corresponds to adding a shunt resistor to ground of value ε at every node or grounding a network with $n+1$ nodes. Aside from circuits, natural applications of grounded Laplacian matrices are networks with reference nodes as in opinion dynamics with stubborn agents [109], [153], distributed estimation with partial measurements

[10], or platooning of vehicles [76]. The grounded Laplacian $\mathcal{L}_{\text{ground}}$ is also an interesting algebraic graph and matrix theory concept in its own right and studied in [100], [69].

Non-singular circuit equations: In case that G has at least one positive diagonal entry, then $-(\mathcal{L}+G)$ is a Hurwitz Metzler matrix, as discussed in Section III-7 and Appendix A. The solution to (18) is therefore unique, and is given by

$$V = (\mathcal{L}+G)^{-1} I\,. \tag{24}$$

The matrix $\mathcal{L}+G$ is sometimes called a *loopy Laplacian matrix* since the non-zero diagonal entry represents a self-loop in the graph [52]. This matrix can also be thought of as the grounded Laplacian matrix of an appropriate $(n+1)\times(n+1)$-dimensional Laplacian matrix [52]. Since $-(\mathcal{L}+G)$ is Metzler, Hurwitz, and irreducible, then we know from Section III-7 that $(\mathcal{L}+G)^{-1}$ is a positive matrix. An important consequence is that if the current injections I in (24) are nonnegative with at least one strictly positive injection, then the unique voltage solution V is a strictly positive vector; this is in contrast to the singular case (19). For example, this occurs if the current injections I arise from converting voltage sources into current sources (Section IV-A6). The matrices $\mathcal{L}_{\text{reg}}$, $\mathcal{L}_{\text{ground}}$, $\mathcal{L}_{\text{shunt}}$, and $(\mathcal{L}+G)$ are all positive definite, and their inverses can be further characterized in terms of their so-called decay properties [46], [15], [100]. These decay properties reveal that the effect a current injection I_i at node i on the potential V_j of another node j diminishes according to the distance between nodes i and j; we now explore this distance concept further.

2) The effective resistance and its properties: Consider an undirected, connected, and weighted graph and an associated connected resistive electrical network governed by the equations (18) with $G = \mathbb{0}_{n\times n}$. The *effective resistance* r_{ij}^{eff} between any pair of (not necessarily neighboring) nodes $i,j \in \{1,\dots,n\}$ is defined as the potential difference $V_i - V_j$ between these nodes when a unit current is injected into node i and extracted from node j; see Figure 15 for an illustration.

For the example in Figure 5 the effective resistance between nodes 1 and 3 takes the well-known value $r_{13}^{\text{eff}} = r_{13}^{\text{red}} = r_{12} + r_{23}$ sometimes referred to as reduced or equivalent resistance.

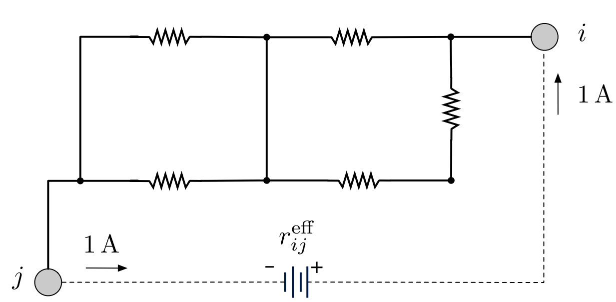

Fig. 15. The effective resistance between nodes i and j is the potential difference when a unit current of 1 A is injected in i and extracted in j.

Note that the potential difference between nodes i and j is $(\mathbb{e}_i - \mathbb{e}_j)^\mathsf{T} V$, the current injection takes the form $I = \mathbb{e}_i - \mathbb{e}_j = \mathcal{L}V$, and accordingly $V = \mathcal{L}^\dagger(\mathbb{e}_i - \mathbb{e}_j)$ from (19). From these simple facts we obtain the following result.

Proposition 5.2 (Effective resistance): The effective resistance r_{ij}^{eff} between two nodes $i,j \in \{1,\dots,n\}$ of an undirected, connected, and weighted graph with Laplacian matrix $\mathcal{L}$ is given by

$$r_{ij}^{\text{eff}} = (\mathbb{e}_i - \mathbb{e}_j)^\mathsf{T} \mathcal{L}^\dagger (\mathbb{e}_i - \mathbb{e}_j) = \mathcal{L}_{ii}^\dagger + \mathcal{L}_{jj}^\dagger - 2\mathcal{L}_{ij}^\dagger\,. \tag{25}$$

We remark that the effective resistance and all of its properties derived below can be obtained analogously if $G \neq \mathbb{0}_{n\times n}$ or with the regularized or grounded Laplacian matrices [52]. The effective resistance is also referred to as the *resistance distance* [88] since it defines a distance metric on a graph (it is symmetric, nonnegative, and satisfies the triangle inequality).

Proposition 5.3 (Effective resistance is a distance [88]): Consider an undirected, connected, and weighted graph with n nodes. The associated *effective resistances* r_{ij}^{eff} satisfy

(i) nonnegativity: $r_{ij}^{\text{eff}} \geq 0$ for all $i,j \in \{1,\dots,n\}$ and $r_{ij}^{\text{eff}} = 0$ if and only if $i = j$;
(ii) symmetry: $r_{ij}^{\text{eff}} = r_{ji}^{\text{eff}}$ for all $i,j \in \{1,\dots,n\}$; and
(iii) triangle inequality: $r_{ij}^{\text{eff}} \leq r_{ik}^{\text{eff}} + r_{kj}^{\text{eff}}$ for all $i,j,k \in \{1,\dots,n\}$.

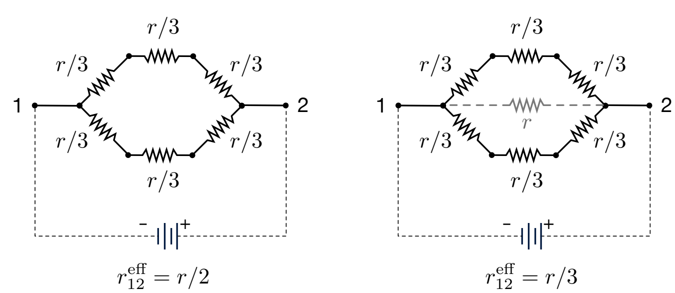

Fig. 16. Adding an edge to the circuit in the panel lowers the effective resistance between nodes $\{1,2\}$ in the circuit in the right panel. In other words, the effective resistance takes parallel paths into account and is a monotonically non-increasing function of topology and weights.

Compared to other distance metrics on graphs, e.g., the topological distance given by the length of the shortest (possibly weighted) path between nodes [72], the effective resistance takes into account all parallel paths. For example, in the left panel of Figure 16, nodes 1 and 2 are connected by two parallel paths each of resistance r. They have a resistance distance $r_{ij}^{\text{eff}} = r/2$ whereas the weighted shortest path takes the value r. Hence, the effective resistance is the preferred distance metric in electrical networks, e.g., see [40], and also in non-technological applications where parallel paths need to be taken into account such as chemistry [81], ecology [96], and disease spreading [2], amongst others.

Related to these parallel paths is the fact that the effective resistance characterizes an *average performance* measure for random walks in Markov chains [55], distributed estimation [10], average consensus [156], [92], and other diffusive graph algorithms [61]; see also Proposition 5.11. Indeed, compared to worst-case performance measures related to dominant eigenvalues of adjacency and Laplacian matrices, the sum of all effective resistances is related to the harmonic mean of all non-zero Laplacian eigenvalues.

Proposition 5.4 (Effective resistance and Laplacian eigenvalues [154]): Consider an undirected, connected, and weighted graph with n nodes, its Laplacian matrix $\mathcal{L} \in \mathbb{R}^{n\times n}$ with spectrum $\text{spec}(\mathcal{L}) = \{0, \lambda_2, \dots, \lambda_n\}$, its effective resistances r_{ij}^{eff} in (25) for all $i, j \in \{1, \dots, n\}$, and define the total effective resistance as $R_{\text{tot}} = \sum_{i,j=1,i<j}^{n} r_{ij}^{\text{eff}}$. It holds that

$$R_{\text{tot}} = \sum_{i,j=1,i<j}^{n} r_{ij}^{\text{eff}} = n \sum_{i=2}^{n} \frac{1}{\lambda_i}\,. \tag{26}$$

Another important property of the effective resistance is *Rayleigh's monotonicity law* stating that the effective resistances are monotonically increasing functions of the branch resistances, e.g., compare the two networks and effective resistances in Figure 16. We state Rayleigh's monotonicity law in the language of algebraic graph theory below.

Proposition 5.5 (Rayleigh's monotonicity law [55]): Consider two symmetric and irreducible adjacency matrices $A, \tilde{A} \in \mathbb{R}^{n\times n}$ corresponding to two undirected, connected, and weighted graphs with identical node sets but possibly different edge sets and edge weights. Consider the associated effective resistances r_{ij}^{eff} and $\tilde{r}_{ij}^{\text{eff}}$ for $i, j \in \{1, \dots, n\}$. If $\tilde{A}_{ij} \geq A_{ij}$ for all $i, j \in \{1, \dots, n\}$, then $\tilde{r}_{ij}^{\text{eff}} \leq r_{ij}^{\text{eff}}$ for all $i, j \in \{1, \dots, n\}$.

Aside from this important monotonicity property exploited in many algorithmic applications, the effective resistance is also known to be a strictly convex function of the graph weights [70]. The latter fact makes the effective resistance attractive for circuit design as well as the synthesis and tuning of diffusive algorithms leveraging the analogy to electrical networks [55], [10], [156], [70], [92].

In conclusion, the effective resistance is motivated from electrical networks, but it has now a firm place in graph theory and its applications. We refer to [55], [154], [88], [52], [10], [70], [69], [157], [75], [61] for further exploration of the rich literature.

3) Network Kron reduction: We revisit the series circuit contraction and the star-triangle transformation from Subsection II-D and analyze them through algebraic graph theory.

Consider again the connected and resistive electrical network model (18), and assume for simplicity here that $G = \mathbb{0}_{n\times n}$. We partition the nodes into two sets $\{1, \dots, n\} = \mathcal{U}_1 \cup \mathcal{U}_2$ that we term boundary nodes $\mathcal{U}_1$ and interior nodes $\mathcal{U}_2$, e.g., $\mathcal{U}_1 = \{1, 3\}$ and $\mathcal{U}_2 = \{2\}$ for the series circuit in Figure 5 and $\mathcal{U}_1 = \{1, 2, 3\}$ and $\mathcal{U}_2 = \{4\}$ for the star in Figure 6. The associated partitioned current-balance equations (18) are

$$\left[\begin{array}{c} I_1 \\ \hline I_2 \end{array}\right] = \left[\begin{array}{c|c} \mathcal{L}_{11} & \mathcal{L}_{12} \\ \hline \mathcal{L}_{12}^{\mathsf{T}} & \mathcal{L}_{22} \end{array}\right] \left[\begin{array}{c} V_1 \\ \hline V_2 \end{array}\right]. \tag{27}$$

Observe that the lower-right block $\mathcal{L}_{22}$ is a loopy Laplacian matrix and is thus (as we observed in Section V-A1) nonsingular. By eliminating the voltages V_2 of the interior nodes as $V_2 = \mathcal{L}_{22}^{-1} I_2 - \mathcal{L}_{22}^{-1}\mathcal{L}_{12}^{\mathsf{T}} V_1$, we obtain the reduced model

$$\underbrace{I_1 - \mathcal{L}_{12}\mathcal{L}_{22}^{-1} I_2}_{I^{\text{red}}} = \underbrace{\left(\mathcal{L}_{11} - \mathcal{L}_{12}\mathcal{L}_{22}^{-1}\mathcal{L}_{12}^{\mathsf{T}}\right)}_{\mathcal{L}^{\text{red}}} V_1\,, \tag{28}$$

where I^{red} and $\mathcal{L}^{\text{red}}$ can be interpreted as reduced current injections and reduced conductance matrix, respectively. This algebraic elimination procedure is termed *Kron reduction* after Gabriel Kron [89]. The reader is invited to verify that the well-known transformations in Subsection II-D are special cases of Kron reduction, and so are many related circuit transformations [142], [117], [115]. An application to a power system model is shown in Figure 17. In the following, we establish that the Kron-reduced equations (28) indeed define an electrical network, as suggested by the examples in Figures 5 and 6.

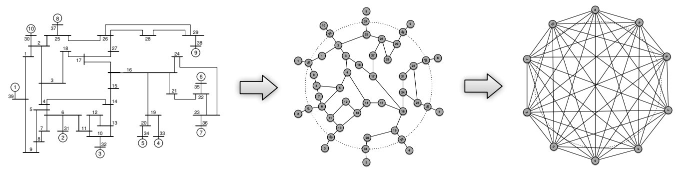

Fig. 17. Illustration of the IEEE 39 New England power system [105] with generator nodes $\{1, \dots, 10\}$ depicted as circles on the left panel; graph-theoretic abstraction in the middle panel with nodes $\{1, \dots, 10\}$ outside the dashed circle; and the Kron-reduced network reduced to nodes $\{1, \dots, 10\}$.

Proposition 5.6 (Kron reduction [132], [52]): Consider the resistive network equations (27) parameterized by the irreducible conductance matrix $\mathcal{L} \in \mathbb{R}^{n\times n}$ satisfying $\mathcal{L}\mathbb{1}_n = \mathbb{0}_n$ and the balanced current injections $I \in \mathbb{R}^n$ satisfying $\mathbb{1}_n^{\mathsf{T}} I = 0$. Consider also the associated Kron-reduced network equations (28) parameterized by the reduced injections I^{red} and conductance matrix $\mathcal{L}^{\text{red}}$. The following statements hold:

(i) The matrix $-\mathcal{L}_{12}\mathcal{L}_{22}^{-1}$ is nonnegative and column-stochastic, and thus the reduced current injections $I^{\text{red}} = I_1 - \mathcal{L}_{12}\mathcal{L}_{22}^{-1} I_2$ are balanced: $\mathbb{1}^{\mathsf{T}} I^{\text{red}} = 0$.

(ii) The reduced conductance matrix $\mathcal{L}^{\text{red}} = \mathcal{L}_{11} - \mathcal{L}_{12}\mathcal{L}_{22}^{-1}\mathcal{L}_{12}^{\mathsf{T}}$ is a nonnegative, symmetric, and irreducible Laplacian matrix satisfying $\mathcal{L}^{\text{red}}\mathbb{1} = \mathbb{0}$.

Now that we have established that Kron reduction is well-posed and defines an electrical network, we are interested in its graph-theoretic properties. We begin by studying the topology and weights of the Kron-reduced network. Observe from the examples in Figures 5, 6, and 17 that the graph associated to the Kron-reduced network is always *denser* than the original graph both in terms of topology and weights. This statement can be made precise as follows.

Proposition 5.7 (Graph-theoretical properties of Kron reduction [52]): Consider the network equations (27) and the Kron-reduced equations (28) with conductance matrices $\mathcal{L}$ and $\mathcal{L}^{\text{red}}$, respectively. The graph associated to the conductance matrix $\mathcal{L}^{\text{red}}$ has an edge between boundary nodes $i, j \in \mathcal{U}_1$ if and only if either

- $\{i, j\}$ is an edge in the original graph associated to the conductance matrix $\mathcal{L}$, or
- there is a path $\{i, k_1, \dots, k_m, j\}$ in the original graph between nodes i and j passing through only interior nodes $\{k_1, \dots, k_m\} \subset \mathcal{U}_2$.

Moreover, for all distinct $i, j \in \mathcal{U}_1$, it holds that $\mathcal{L}_{ij}^{\text{red}} \leq \mathcal{L}_{ij}$, that is, the weights are non-decreasing.

A consequence of Proposition 5.7 is the following characterization that is intuitive from the Y-Δ transformation in

Figure 6: if a set of interior nodes $\kappa \subseteq \mathcal{U}_2$ forms a connected subgraph in the original network, then the boundary nodes adjacent to κ form a clique in the Kron-reduced network.

The careful reader may have observed that the series contraction in Figure 5 is an instance of Kron reduction network where the reduced resistance takes the same value as the effective resistance between nodes 1 and 3: $r_{13}^{\text{red}} = r_{12} + r_{23} = r_{13}^{\text{eff}}$. In general, the Kron-reduced matrix and the effective resistance admit such a direct relationship only in very uniform networks; see [52] for details. However, it is always true that the effective resistance is invariant under Kron reduction.

Proposition 5.8 (Invariance of effective resistance [52]): Consider the network model (27) and the Kron-reduced model (28) with conductance matrices $\mathcal{L}$ and $\mathcal{L}^{\text{red}}$, respectively. Then for any boundary nodes $i, j \in \mathcal{U}_1$, the effective resistances r_{ij}^{eff} can be equivalently computed from $\mathcal{L}$ or $\mathcal{L}^{\text{red}}$:

$$r_{ij}^{\text{eff}} = (\mathbb{e}_i - \mathbb{e}_j)^\top \mathcal{L}^\dagger (\mathbb{e}_i - \mathbb{e}_j) = (\mathbb{e}_i - \mathbb{e}_j)^\top \left(\mathcal{L}^{\text{red}}\right)^\dagger (\mathbb{e}_i - \mathbb{e}_j) .$$

We remark that all of the above results on Kron reduction can be adapted to the case when the network features shunt resistors ($G \neq \mathbb{0}_{n\times n}$), and related topological, spectral, and algebraic properties can be derived; see [52] for further details.

The graph-theoretic perspective on Kron reduction finds direct application in the synthesis and analysis of circuits [132], [136], [150] particularly in the context of large-scale integration chips [113], [3], power system and power electronics model reduction [143], [94], [28], [47], [129], smart grid monitoring [48], [123], electrical impedance tomography [23], [41], and many other domains of electrical networks. In a general context, algebraic equations governed by Laplacian matrices such as (18) are encountered in many scientific disciplines. Thus, Kron reduction can be found under different names and with a graph-theoretic perspective in Gaussian elimination of sparse matrices [65], [71], [114], sparse grid and finite-element solvers [139], [43], [138], statistical mechanics [107], data mining [155], [69], reduction of Markov chains [98], [18], signal processing on graphs [108], [159], and pure algebraic graph theory [66], [62], [125] among others.

We conclude by remarking that this rich literature dating back to the early days of electrical circuits is still active today. Many applications and graph-theoretic properties are still to be explored. Even apparently simple extensions to directed and complex-valued graphs (as occurring later in Section VI-B) are mostly open to the best of our knowledge; see the concluding Section VII or, e.g., the recent article [134] discussing classical and open problems in linear resistive networks.

B. Dynamic resistive-capacitive (RC) networks

Now that we have thoroughly examined static resistive networks, we move on towards dynamic RC networks with the first-order dynamics (12) in the linear setting when $P^* = \mathbb{0}_n$:

$$C\dot{V}(t) = -\left(\mathcal{L} + G\right) V(t) + I^* . \tag{29}$$

We will assume that C is a diagonal and positive definite matrix of capacitances, and the conductance matrix $\mathcal{L}$ is an irreducible Laplacian matrix. Consider first the dissipative case when G has at least one strictly positive diagonal element. In this case, the associated compartmental system is outflow-connected (see Appendix A and Section II-B), and the matrix $-C^{-1}\left(\mathcal{L} + G\right)$ is Metzler, Hurwitz, and irreducible. The following proposition summarizes this discussion.

Proposition 5.9 (Stability of dissipative RC network): Consider the dissipative RC network dynamics (29) and assume that G has at least one strictly positive diagonal element. Then from every initial voltage profile $V(t=0)$, the dynamics (29) converge exponentially to the unique equilibrium voltage profile

$$\lim_{t\to\infty} V(t) = \left(\mathcal{L} + G\right)^{-1} I^* .$$

Next, consider the case without shunt conductances when $G = \mathbb{0}_{n\times n}$:

$$C\dot{V}(t) = -\mathcal{L} V(t) + I^* . \tag{30}$$

Recall from Section V-A that the network dynamics (30) admit an equilibrium as in (19) if and only if $\mathbb{1}_n^\top I^* = 0$. To further characterize the degree of freedom $\alpha \in \mathbb{R}$ of the equilibrium (19), note that the total charge is conserved:

$$\frac{\mathrm{d}}{\mathrm{d}t}\left(\mathbb{1}_n^\top C V\right) = \mathbb{1}_n^\top I^* = 0 , \tag{31}$$

where we have used the fact that $\mathbb{1}_n^\top \mathcal{L} = \mathbb{0}_n^\top$. Accordingly, $\mathbb{1}_n^\top C V(t) = \mathbb{1}_n^\top C V_0$ for all $t \geq 0$, where $V_0 = V(t=0)$. It follows by substituting (19) into this conservation law that

$$\alpha = \frac{\mathbb{1}_n^\top C (V_0 - \mathcal{L}^\dagger I^*)}{\mathbb{1}_n^\top C \mathbb{1}_n} . \tag{32}$$

To show stability of the equilibrium profile (19) with α as in (32), we define the voltage error coordinate

$$\tilde{V} = V - \alpha \mathbb{1}_n - \mathcal{L}^\dagger I^* , \tag{33}$$

and a quick calculation (making use of Proposition 5.1) shows that $\tilde{V}$ satisfies the differential equation $C\dot{\tilde{V}} = -\mathcal{L}\tilde{V}$. Consider now the energy-like function $W(\tilde{V}) = \frac{1}{2}\tilde{V}^\top C \tilde{V}$. It can be verified that this energy is non-increasing along trajectories:

$$\frac{\mathrm{d}}{\mathrm{d}t} W(\tilde{V}) = -\tilde{V}^\top \mathcal{L} \tilde{V} \leq -\lambda_2 \|\tilde{V}\|^2 \leq -\frac{\lambda_2}{c_{\max}} W(\tilde{V}) , \tag{34}$$

where λ_2 is the second-smallest eigenvalue of the Laplacian matrix known as the *algebraic connectivity*; see Section III-6. From this so-called dissipation inequality [147], we obtain the exponential decay estimate $W(\tilde{V}(t)) \leq W(\tilde{V}_0)\exp(-\frac{\lambda_2}{c_{\max}} t)$, which again implies that $\tilde{V}(t)$ converges exponentially:

$$\left\|\tilde{V}(t)\right\| \leq \left\|\tilde{V}_0\right\| \frac{c_{\max}}{c_{\min}} \exp\left(-\frac{\lambda_2}{2c_{\max}} t\right) . \tag{35}$$

This discussion is summarized in the following proposition.

Proposition 5.10 (Stability of RC network without shunt conductances): Consider the RC network dynamics (30) without shunt conductances and assume that $\mathbb{1}_n^\top I^* = 0$. Then for every initial voltage profile $V_0 \in \mathbb{R}^n$, the dynamics converge to the unique and exponentially stable equilibrium voltage profile

$$\lim_{t\to\infty} V(t) = \alpha \mathbb{1}_n - \mathcal{L}^\dagger I^* ,$$

where α is given by (32). The convergence is exponential with a decay rate proportional to λ_2 as in (35). Moreover, the total charge is conserved along solutions as in (31).

The following remarks are in order. In the absence of external injections, $I^* = \mathbb{0}_n$, the voltages equalize to the flat profile $\frac{\mathbb{1}_n^\top C V_0}{\mathbb{1}_n^\top C \mathbb{1}_n}\mathbb{1}_n$; this constant uniform voltage is a weighted average of the initial voltage values, with weights depending on the capacitances. The features of the particular solution $\mathcal{L}^\dagger I^*$ have been discussed in detail in Section V-A. The voltage error coordinate (33) is related to the disagreement vector studied in consensus problems [103], [33]. The exponential decay estimate $\lambda_2/c_{\max}$ in (35) depends on the maximum capacitance as well as on the algebraic connectivity λ_2 of the network. The algebraic connectivity is a well-studied quantity in algebraic graph theory dating back to the seminal work by Fiedler [64]. For example, λ_2 is a popular metric in graph partitioning and community detection [111], [67] as it quantifies the smallest bottleneck in the graph, where "smallest" is understood in our context as the minimal current flow over any cut separating the nodes of an electrical network.

The exponential decay estimate (35) is achieved for a *worst-case* initial condition $\tilde{V}_0$ aligned with the eigenvector v_2 associated to the eigenvalue λ_2. However, often one is interested in an *average* integral-quadratic performance criterion

$$\mathbb{E}\left[\int_0^\infty \tilde{V}(t)^\top \Pi_n \tilde{V}(t)\, dt\right], \tag{36}$$

where the expectation is with respect to a random initial error voltage profile $\tilde{V}_0$ with zero mean and $\mathbb{E}\big[\tilde{V}_0\tilde{V}_0^\top\big] = \Pi_n$ (possibly due to a random realization of the current demands I or initial voltages V_0). The projector matrix Π_n induces the global voltage error $\tilde{V}^\top \Pi_n \tilde{V} = \|\tilde{V} - \text{average}(\tilde{V})\mathbb{1}_n\|^2$, and discards values of $\tilde{V}(t)$ and $\tilde{V}_0$ aligned with $\mathbb{1}_n$ that do not affect the transient dynamics. The integral quadratic performance metric criterion (36) is well-known in control and signal processing under the name of an $\mathcal{H}_2$-norm of a system [161], and it is well-studied for the system (30) in the context of consensus systems [29], [7], [156], power systems [126], [110], and random walks [55], [69], among others. In our case and for identical capacitors $C = I_n$, the average performance criterion (36) evaluates to an average of the inverse non-zero Laplacian eigenvalues as in the total effective resistance (26).

Proposition 5.11 (Average performance of RC network [27]): Consider the RC network dynamics (30) with identical capacitors $C = I_n$, the voltage error coordinate (33), and the average integral quadratic performance criterion (36) for a random initial condition $\tilde{V}_0 \in \mathbb{R}^n$ with zero mean and $\mathbb{E}\big[\tilde{V}_0\tilde{V}_0^\top\big] = \Pi_n$. The performance criterion (36) evaluates to

$$\mathbb{E}\left[\int_0^\infty \tilde{V}(t)^\top \Pi_n \tilde{V}(t)\, dt\right] = \sum_{i=2}^{n} \frac{1}{\lambda_i} = R_{\text{tot}}/n\,, \tag{37}$$

where R_{tot} is the total effective resistance (26).

There are several equivalent interpretations of the $\mathcal{H}_2$-norm (36) aside from characterizing the average convergence rate (37) [161]. For example, an equivalent interpretation is the steady-state voltage variance when subjecting each node to noisy current inputs or the transient energy dissipated by the circuit after being subjected to impulsive current inputs arising, e.g., from line faults [38], [126]. While admittedly, the average performance index (36) is of minor importance to circuits, it plays a key role in the design of distributed algorithms with diffusive dynamics [29], [7], [156], [55], [69], [92], [61], where the analogy to the effective resistance provides important intuition, and well-known concepts on the electrical side (such as Rayleigh's monotonicity law) inspire and inform the design and analysis of algorithms. Finally, we remark that the above result can be extended to more general cost functions than (36), higher-order dynamics, and discrete-time settings [29], [7], [156], [110], [38], [130], [38], [130]. Extensions to nonlinear circuits remain an open problem.

C. Dynamic resistive-inductive-capacitive (RLC) networks

In this section we analyze the full RLC network model (11) from Section IV-C, repeated here for convenience:

$$\begin{bmatrix} C & \\ & L \end{bmatrix}\begin{bmatrix} \dot{V} \\ \dot{f} \end{bmatrix} = \begin{bmatrix} -G & -B \\ B^\top & -R \end{bmatrix}\begin{bmatrix} V \\ f \end{bmatrix} + \begin{bmatrix} I^* + P^* \oslash V \\ \mathbb{0}_m \end{bmatrix}.$$

Our approach will be to leverage the algebraic graph theory methods introduced in Section III. We begin by highlighting the energy conservation and dissipation properties of the network system (11). Consider the electric and the magnetic energy associated to the network storage elements:

$$\mathcal{H}(V, f) = \frac{1}{2}V^\top C V + \frac{1}{2} f^\top L f\,. \tag{38}$$

The time derivative of the energy (38) along trajectories of the network dynamics (11) is given by the *power balance*

$$\dot{\mathcal{H}}(V,f) = \underbrace{\begin{bmatrix} V \\ f \end{bmatrix}^\top \begin{bmatrix} & -B \\ B^\top & \end{bmatrix}\begin{bmatrix} V \\ f \end{bmatrix}}_{=0 \text{ (lossless power circulations)}} \underbrace{-\begin{bmatrix} V \\ f \end{bmatrix}^\top \begin{bmatrix} G & \\ & R \end{bmatrix}\begin{bmatrix} V \\ f \end{bmatrix}}_{\leq 0 \text{ (power losses)}} \underbrace{+V^\top I^* + \mathbb{1}_n^\top P^*}_{\text{(external power supplied)}}, \tag{39}$$

where we used the identity $V^\top(P^* \oslash V) = \mathbb{1}_n^\top P^*$. The last term in the power balance equation (39) corresponds to the external power supplied to the network through the external current and power injections, the central term corresponds to dissipation induced by shunt and branch resistances, and the first term evaluates to zero due to skew-symmetry of matrix in the quadratic form. To further understand the role of the first term, consider the network (14) without branch dissipation $R = \mathbb{0}$ and without loads ($G = \mathbb{0}, I^* = P^* = \mathbb{0}_n$). In this case, the total energy is preserved $\dot{\mathcal{H}}(V,f) = 0$, and thus $\mathcal{H}(V(t), f(t)) = \mathcal{H}(V_0, f_0)$ for all $t \geq 0$, which says the ellipsoidal level sets of the energy function (38) are invariant. In particular, since the system (14) is linear, these level sets are the images of oscillating harmonic trajectories $(V(t), f(t))$. Thus, the dynamic behavior of the lossless network (14) and the first term in the general power balance (39) correspond to lossless energy exchange (i.e., power circulations) between the inductive and capacitive storage elements. For identical time constants $C = I_n$, the dynamics (14) reduce to the *Laplacian oscillator* (15) and the solutions can be further characterized.

Proposition 5.12 (Circulations in lossless circuit [49]): Consider the lossless network model (14). The solution is a superposition of n undamped harmonic signals. Moreover, if $C = I_n$, then the frequencies† of these harmonic signals are $\sqrt{\lambda_i}$, $i \in \{1, \dots, n\}$, where λ_i are the eigenvalues of the L^{-1}-weighted Laplacian matrix $\mathcal{L}_L = BL^{-1}B^\top$.

The power balance equation (39) is a special case of a so-called dissipation (in)equality (more specifically a passivity inequality) [147], [131], and the insights gained from it lay the foundations for further analysis of general nonlinear electrical networks [95], [128] and other interconnected systems [133], [135], [104]. For example, another key insight is that, for positive definite matrices G and R, the right-hand side of (39) is strictly negative for sufficiently large values of voltages V and currents f. It follows that in this case, the trajectories of the nonlinear network dynamics (11) are always bounded. Notice also that the analysis of linear RC circuits, treated previously in Subsection V-B, can be equivalently performed based on matrix theory or dissipation inequalities such as (34).

We will defer a further nonlinear analysis to Section VI-A and focus now on the linear and homogeneous case when $P^* = I^* = \mathbb{0}_n$ to showcase the tools of algebraic graph theory from Section III. Consider the network dynamics

$$\begin{bmatrix} C & \\ & L \end{bmatrix} \begin{bmatrix} \dot{V} \\ \dot{f} \end{bmatrix} = \underbrace{\begin{bmatrix} -G & -B \\ B^\top & -R \end{bmatrix}}_{=\mathcal{A}} \begin{bmatrix} V \\ f \end{bmatrix}. \tag{40}$$

The network matrix $\mathcal{A}$ is related to so-called saddle or KKT matrices [14] in quadratic optimization programs with linear equality constraints (where $R = \mathbb{0}$). We collect some properties in the following proposition that is proved in Appendix B.

Proposition 5.13 (Spectrum of saddle matrices): Consider the network matrix $\mathcal{A}$ in (40), where G and R are positive semidefinite, and the graph associated to the incidence matrix B is connected. The matrix $\mathcal{A}$ has the following properties:

1) all eigenvalues are in the closed left half-plane: $\mathrm{spec}(\mathcal{A}) \subset \{\lambda \in \mathbb{C} \mid \Re(\lambda) \leq 0\}$. Moreover, all eigenvalues on the imaginary axis have equal algebraic and geometric multiplicities;
2) if G and R are zero matrices, then all eigenvalues of $\mathcal{A}$ are on the imaginary axis and $\mathrm{spec}(\mathcal{A}) = \{0, 0, \pm i\lambda_2, \dots, \pm i\lambda_n\}$, where $\{\lambda_2, \dots, \lambda_n\}$ are the non-zero eigenvalues of the unweighted Laplacian $BB^\top$;
3) if G and R are positive definite, then $\mathcal{A}$ is Hurwitz;
4) if $\mathrm{Ker}(G) \cap \mathrm{Im}(B) = \{\mathbb{0}_n\}$, then $\mathcal{A}$ has no eigenvalues on the imaginary axis except for 0. Moreover, if G is positive definite and B has full rank (i.e., the graph is acyclic), then $\mathcal{A}$ is Hurwitz; and
5) if $\mathrm{Ker}(R) \cap \mathrm{Im}(B^\top) = \{\mathbb{0}_n\}$, then $\mathcal{A}$ has no eigenvalues on the imaginary axis except for 0. Moreover, if R is positive definite and $G_{ii} > 0$ for at least one element $i \in \{1, \dots, n\}$, then $\mathcal{A}$ is Hurwitz.

The above matrix spectrum results for $\mathcal{A}$ translate quickly into dynamic stability results for the system (40), since the inductances and capacitances L and C do not change the stability of $\mathcal{A}$ (which can be seen, e.g., by changing coordinates to $\begin{bmatrix} C^{\frac{1}{2}} V & L^{\frac{1}{2}} f \end{bmatrix}$). Property 1) guarantees that the dynamics (40) are always marginally stable, possibly with sustained oscillations or constant non-decaying modes. Whenever G (respectively, R) is positive definite, then property 4) (respectively, property 5)) guarantees that no sustained oscillations can occur. However, in this case it is not true that all signals will necessarily settle to zero. For example, assume that that G is positive definite and $R = \mathbb{0}$; this satisfies the assumptions of property 4). Then a possible equilibrium for (40) is

$$V^* = \mathbb{0}_n , \qquad f^* \in \mathrm{Ker}(B) ,$$

that is, the equilibrium current flows f^* live in the cycle space $\mathrm{Ker}(B)$ of the graph; see Section III-9. Hence, any initial current circulation $f_0 \in \mathrm{Ker}(B)$ is persistent and does not dissipate. Of course, this is ruled out if either B has full rank (i.e., the graph is acyclic) or R is positive definite so that dissipation forces all circulating flows vanish. Similarly, in the scenario of property 5) with $G = \mathbb{0}_{n\times n}$ and R positive definite, we observe that a possible equilibrium is

$$V^* \in \mathrm{Ker}(B^\top) = \mathrm{span}(\mathbb{1}_n) , \qquad f^* = \mathbb{0}_m ,$$

which allows for any uniform potential vector V^* analogous to the conservation of charge in (33). If at least one shunt resistance $G_{ii} > 0$ is present, then dissipation forces $V^* = \mathbb{0}_n$.

Several of the special cases we have considered thus far allow for a more detailed analysis of the linear network dynamics (40). In particular, recall the Laplacian oscillator dynamics (15) analyzed in Proposition 5.12, the homogeneous network dynamics (16), and the coupled ℓc-tanks (17) in Figure 2. These dynamics are all instances of the more general *second-order Laplacian flow*

$$\ddot{V} + (k_{\mathrm{d}} I_n + \gamma_{\mathrm{d}} \mathcal{L})\dot{V} + (k_{\mathrm{p}} I_n + \gamma_{\mathrm{p}} \mathcal{L})V = \mathbb{0}_n, \tag{41}$$

which can be written in state-space form as

$$\frac{\mathrm{d}}{\mathrm{d}t} \begin{bmatrix} V \\ \dot{V} \end{bmatrix} = \underbrace{\begin{bmatrix} \mathbb{0}_{n\times n} & I_n \\ -k_{\mathrm{p}} I_n - \gamma_{\mathrm{p}} \mathcal{L} & -k_{\mathrm{d}} I_n - \gamma_{\mathrm{d}} \mathcal{L} \end{bmatrix}}_{=\mathcal{Q}} \begin{bmatrix} V \\ \dot{V} \end{bmatrix} , \tag{42}$$

where $\mathcal{L} \in \mathbb{R}^{n\times n}$ is an irreducible and symmetric Laplacian matrix, and k_{d}, k_{p}, γ_{d}, and γ_{p} are scalar and nonnegative gains that (if positive) induce a diffusive coupling or a resistive dissipation on the voltages V and their drifts $\dot{V}$, respectively.

The dynamics (42) can be elegantly analyzed via a change of coordinates $V \to \mathbb{V}V$, where $\mathbb{V} = \begin{bmatrix} \frac{1}{\sqrt{n}}\mathbb{1}_n & v_2 & \dots & v_n \end{bmatrix}$ collects the eigenvectors of the Laplacian matrix $\mathcal{L}$ as in Proposition 5.1. In these coordinates and after permuting the entries appropriately, the matrix $\mathcal{Q}$ governing the second-order Laplacian flow (42) is similar to a block-diagonal matrix with n blocks, each of the form

$$\begin{bmatrix} 0 & 1 \\ -k_{\mathrm{p}} - \gamma_{\mathrm{p}}\lambda_i & -k_{\mathrm{d}} - \gamma_{\mathrm{d}}\lambda_i \end{bmatrix} , \quad i \in \{1, \dots, n\} ,$$

where $0 = \lambda_1 < \lambda_2 \leq \dots \leq \lambda_n$ are the eigenvalues of the Laplacian matrix $\mathcal{L}$. We can draw the following conclusions.

†Note that the 1st mode $\lambda_1 = 0$ corresponding to average$(V(t))$ results in *constant* (0-frequency) average voltage since $\frac{\mathrm{d}}{\mathrm{d}t}$ average$(V(t)) = 0$.

Proposition 5.14 (Second-order Laplacian flows [27]): Consider the second-order Laplacian flow (42), where $\mathcal{L} \in \mathbb{R}^{n\times n}$ is an irreducible and symmetric Laplacian matrix and $k_{\rm d}, k_{\rm p}, \gamma_{\rm d}, \gamma_{\rm p} \geq 0$ are scalar and nonnegative gains. The following statements hold.

1) given the eigenvalues λ_i, $i \in \{1,\dots,n\}$, of $\mathcal{L}$, the $2n$ eigenvalues $\eta_{i,\pm}$, $i \in \{1,\dots,n\}$, of $\mathcal{Q}$ are solutions to
$$\eta^2 + (k_{\rm d} + \gamma_{\rm d}\lambda_i)\eta + (k_{\rm p} + \gamma_{\rm p}\lambda_i) = 0, \quad i \in \{1,\dots,n\}\,;$$
2) the second-order Laplacian flow (42) achieves a consensus on a voltage profile, that is, $|V_i - V_j| \to 0$ and $|\dot{V}_i - \dot{V}_j| \to 0$ as $t \to \infty$ for all $i,j \in \{1,\dots,n\}$ if and only if the $2(n-1)$ eigenvalues $\eta_{i,\pm}$, $i \in \{2,\dots,n\}$, of the second-order Laplacian matrix $\mathcal{Q}$ have strictly negative real part; and
3) the average voltage dynamics satisfy
$$\frac{\rm d}{{\rm d}t}\begin{bmatrix}\text{average}(V(t))\\ \text{average}(\dot{V}(t))\end{bmatrix} = \begin{bmatrix}0 & 1\\ -k_{\rm p} & -k_{\rm d}\end{bmatrix}\begin{bmatrix}\text{average}(V(t))\\ \text{average}(\dot{V}(t))\end{bmatrix}.$$

Moreover, if the voltages achieve a consensus on a voltage profile, then the steady-state profile equals the average initial voltage.

We can now interpret the previous dynamics as special cases of Proposition 5.14. For example, the coupled ℓc-tanks (17) in Figure 2 define a second-order Laplacian flow with $k_{\rm p} = \omega_0^2$, $\gamma_{\rm d} = \tau'$, and $k_{\rm d} = \gamma_{\rm p} = 0$. Accordingly, all eigenvalues $\eta_{i,\pm}$, $i \in \{2,\dots,n\}$ of $\mathcal{Q}$ are in the open left-half plane, and the asymptotic dynamics are governed by the average voltage:
$$\frac{\rm d}{{\rm d}t}\begin{bmatrix}\text{average}(V(t))\\ \text{average}(\dot{V}(t))\end{bmatrix} = \begin{bmatrix}0 & 1\\ -\omega_0^2 & 0\end{bmatrix}\begin{bmatrix}\text{average}(V(t))\\ \text{average}(\dot{V}(t))\end{bmatrix}.$$
Observe that the asymptotic dynamics equal those of a single ℓc-tank in isolation. The claimed synchronization of the voltages to the average can be observed in Figure 2. Analogous comments apply to the Laplacian oscillator (15) and the homogeneous network dynamics (16).

We make two closing remarks concerning the analyses of this section. First, similar analyses apply in the presence of exogenous constant current inputs I^* by defining appropriate error coordinates. Second, in the case that all signals are sinusoidal of constant and identical frequency and the underlying circuit is asymptotically stable, the above results can be extended to the *alternating current* (AC) domain by resorting to complex-valued variables (so-called phasors), depicting the amplitude and phase of all signals [4], [37]. Though generally more complex dynamic phenomena (e.g., harmonic resonance) can occur; see Section VI-B and (54) for a steady-state model.

VI. Structure and Dynamics of Nonlinear Electrical Networks

In Section V we restricted our attention to a class of linear circuits, leveraging algebraic graph theory to study static properties of solutions and dynamic stability. While Kirchhoff's current and voltage laws are always linear, nonlinearity arises frequently in circuit analysis for a number of reasons, including but not limited to

(i) nonlinear constitutive relations / circuit elements (e.g., voltage-controlled resistances, diodes, transistors) [37];
(ii) nonlinear load or source models (e.g., constant power loads or converter-interfaced sources) [9]; and
(iii) power-oriented modeling of AC circuits [83], [84], [85].

We do not examine nonlinearities arising from (i) in this article, and refer the interested reader to classic literature such as [151], [37] for various results. Instead, this section examines some specific instances of nonlinearity where the methods of algebraic graph theory continue to provide insights into both circuit solutions and dynamic stability. Section VI-A studies the existence of equilibrium points for the nonlinear RLC model (11) with constant power loads. Section VI-B continues this examination for the case of AC circuits, where all steady-state signals are required to be sinusoidal, leading to a discussion of the AC power flow equations.

A. Dynamic resistive-inductive-capacitive (RLC) networks with constant-power loads

1) Equilibrium analysis: A first challenge when studying nonlinear circuits is that even the existence of constant steady-state operating points is no longer guaranteed. Indeed, the example of Section II-C shows that nonlinear circuits can possess multiple steady-state solutions, or possess no solutions at all. We now extend the arguments of Section II-C to the case of networks. In particular, we return to the nonlinear dynamic model (11), and seek to determine sufficient conditions for the existence and uniqueness of an equilibrium point. The equilibria of (11) are solutions of the nonlinear algebraic equations
$$\mathbb{0}_{n+m} = \begin{bmatrix}-G & -B\\ B^\top & -R\end{bmatrix}\begin{bmatrix}V\\ f\end{bmatrix} + \begin{bmatrix}I^* + P^* \oslash V\\ \mathbb{0}_m\end{bmatrix}. \tag{43}$$
If we assume that R is positive definite, the second equation in (43) may be uniquely solved for $f = R^{-1}B^\top V$. By substituting this expression into the first equation, we obtain the set of n nonlinear equations
$$\mathbb{0}_n = -(\mathcal{L}_R + G)V + I^* + P^* \oslash V\,,$$
where $\mathcal{L}_R = BR^{-1}B^\top$. Note that this is exactly the equilibrium equation for the dynamic RC model (12); when R is positive definite, the two models therefore share the same equilibria. If we assume further that (i) at least one element of G is strictly positive, and that (ii) I^* is nonnegative with at least one strictly positive entry (i.e., a current source), then the equilibria are equivalently determined by
$$V = \underbrace{(\mathcal{L}_R + G)^{-1}I^*}_{V_{I^*}} + (\mathcal{L}_R + G)^{-1}(P^* \oslash V)\,, \tag{44}$$
where V_{I^*} is the solution of the *linear* resistive network studied in Section V-A, and has strictly positive components. We continue by introducing the change of variables
$$\delta = (V - V_{I^*}) \oslash V_{I^*}\,,$$
which is simply the percentage deviation of V from V_{I^*}. The equilibrium equation (44) can then be further rewritten as
$$\delta = F(\delta) = \frac{1}{4}P_{\rm crit}^{-1}(P^* \oslash (\mathbb{1}_n + \delta)), \tag{45}$$

where we defined the *critical power flow matrix*

$$P_{\text{crit}} = \frac{1}{4}\operatorname{diag}(V_{I^*})\,(\mathcal{L}_R + G)\,\operatorname{diag}(V_{I^*}) \in \mathbb{R}^{n\times n}\,. \tag{46}$$

One may verify easily that $-P_{\text{crit}}$ is a Hurwitz Metzler matrix, with the same sparsity pattern as $\mathcal{L}_R$. The equation $\delta = F(\delta)$ in (45) is a *fixed-point equation* for the potential deviation δ, and can be studied using the contraction mapping principle [116, Theorem 9.32]. The following result provides an intuitive condition under which the nonlinear circuit (11) possesses an equilibrium.

Proposition 6.1 (Existence and uniqueness of an equilibrium for nonlinear RLC network): Consider the equilibrium equation (43) associated with the nonlinear circuit network model (11). Assume that R is positive definite, that G has at least one strictly positive entry, and that I^* is element-wise nonnegative with at least one strictly positive entry. If

$$\|P_{\text{crit}}^{-1}\operatorname{diag}(P^*)\|_\infty < 1\,, \tag{47}$$

then (43) possesses a solution (V^*, f^*) with $f^* = R^{-1}B^{\mathsf{T}}V^*$. Moreover, the potentials $V^* = \operatorname{diag}(V_{I^*})(\mathbb{1}_n + \delta^*)$ are close to V_{I^*} in the sense that

$$\|(V^* - V_{I^*}) \oslash V_{I^*}\|_\infty = \|\delta^*\|_\infty \leq \delta_{\max}\,, \tag{48}$$

where

$$\delta_{\max} = \frac{1}{2}\left(1 - \sqrt{1 - \|P_{\text{crit}}^{-1}\operatorname{diag}(P^*)\|_\infty}\right) \in [0, 1/2)\,,$$

and (V^*, f^*) is the only solution satisfying the inequality (48).

The proof of this result is nearly identical to the proof of [121, Theorem 1]. The intuition behind Proposition 6.1 is that for the existence of an equilibrium, the maximum size of the constant power demands P^* must be limited.

Existence/uniqueness conditions similar to (47) have been derived by several authors in the context of power distribution systems [22], [158], [141], [11], [5] and microgrids [120], [122], [13] with constant power loads; [22] gives an interpretation of their condition in terms of the maximum path length in the associated graph. All of these conditions have in common that some measure of the size of the constant power load should be small compared to a measure of the coupling strength in the network, quantified in terms of system impedance and nominal voltage level. For the condition (47) above, the quantity $\|P_{\text{crit}}^{-1}\operatorname{diag}(P^*)\|_\infty$ provides a dimensionless measure of how large P^* is, normalized by the critical power flow matrix P_{crit} defined in (46). When the inequality (47) holds, we are guaranteed the existence of an equilibrium which is close to the solution V_{I^*} studied in Section V-A; in general, there can be many equilibria, there is exactly one equilibrium in the box $\{V \in \mathbb{R}^n \mid \|(V - V_{I^*}) \oslash V_{I^*}\|_\infty \leq \delta_{\max}\}$.

Another useful perspective on the condition (47) comes from studying the linearization of the right-hand side of equilibrium equation (44) around $V = V_{I^*}$ and $P^* = \mathbb{0}_n$. Performing this computation, one finds that

$$V \oslash V_{I^*} \approx \mathbb{1}_n + \frac{1}{4}P_{\text{crit}}^{-1}P^*\,. \tag{49}$$

The condition (47) can therefore be interpreted as restricting the first-order term of the linearized solution at the point $V = V_{I^*}$. Many of the insights developed in Section V-A concerning inverse Laplacian matrices and effective resistance can be leveraged to further characterize the solution. For example, just like the matrix $(\mathcal{L}_R + G)$ studied previously, the matrix P_{crit} is also a loopy Laplacian matrix, but for a graph whose edges have been reweighted using the potentials V_{I^*}. In turn, the inverse matrix P_{crit}^{-1} satisfies a decay property, quantified in terms of the effective resistance in this reweighted graph. It follows from (49) then that to first order, these effective resistances quantify the sensitivity of the potential V_i at node i with respect to the power injection P_j^* at node j. A complete discussion of many of these conclusions in the context of an AC circuit model can be found in [121]. As we will see shortly, the condition (47) is also instrumental in assessing local stability of the associated equilibrium point for the RLC and RC network models.

Finally, we note that convex optimization approaches have recently been devised for assessing the existence of equilibrium points for static and dynamic nonlinear circuits. An optimization formulation exploiting the Metzler structure of the graph matrices is presented in [91]. Linear matrix inequality (LMI) conditions for equilibrium infeasibility (i.e., necessary conditions for equilibrium existence) are presented in [9], [93], and a convex programming approach for certifying feasibility of AC power flow may be found in [56]. To our knowledge however, the presented conditions do not have straightforward graph-theoretic interpretations.

2) Dynamic analysis: Aside from the energy and power analysis in Section V-C, a few further fundamental insights into dynamic stability can be obtained by studying the linearization of the nonlinear circuit model (11) around the solution (V^*, f^*) derived in Proposition 6.1:

$$\begin{bmatrix} C & \\ & L\end{bmatrix}\begin{bmatrix}\delta\dot{V}\\ \delta\dot{f}\end{bmatrix} = \underbrace{\begin{bmatrix} -G - (P^* \oslash (V^* \odot V^*)) & -B \\ B^{\mathsf{T}} & -R\end{bmatrix}}_{=\mathcal{A}(V^*)}\begin{bmatrix}\delta V\\ \delta f\end{bmatrix}. \tag{50}$$

These linearized dynamics (50) are exactly of the form (40) studied previously in Section V-C, and results developed for the network matrix $\mathcal{A}$ in Proposition 5.13 can now be applied to the matrix $\mathcal{A}(V^*)$. Based on the properties of the equilibrium in Proposition 6.1, the following parametric stability condition can be established.

Proposition 6.2 (Local stability of dynamic RLC network): Consider the dynamic RLC network model (11). Assume the conditions of Proposition 6.1 hold, and let V_{I^*} and $\delta_{\max}$ be as in Proposition 6.1. Then the equilibrium point (V^*, f^*) is locally exponentially stable if

$$\tilde{g}_i := g_i + \frac{P_i^*}{(V_{I^*})_i^2(1 - \delta_{\max})^2} \geq 0\,, \quad i \in \{1, \ldots, n\}\,,$$

with strict inequality for at least one value of i.

The proof of this result may be found in Appendix C. The quantity $\tilde{g}_i$ can be interpreted as an effective shunt conductance at node $i \in \{1, \ldots, n\}$, in which the constant power load P_i^* has been converted into a shunt conductance. The stability result may then be seen as a case of item 5) in Proposition

5.13. The effective shunt conductances $\tilde{g}_i$ depend on $\delta_{\max}$, which in turn depends on the key quantity $\|P_{\text{crit}}^{-1}\,\text{diag}(P^*)\|_\infty$ from Proposition 6.1. Stability therefore depends directly on the spectral properties of the graph matrix P_{crit}.

As noted earlier, (V^*, f^*) is an equilibrium point of the RLC model (11) (with R positive definite) if and only if V^* is an equilibrium point of the RC model (12). We can therefore also assess the local stability of the equilibrium point in Proposition 6.1 for the RC model.

Proposition 6.3 (Local stability of dynamic RC network): Consider the dynamic RC network model (12). Assume the conditions of Proposition 6.1 hold, and let V^* be the specified equilibrium point. Then V^* is locally exponentially stable.

The proof of this result may be found in Appendix D. To conclude this section, we now examine some large-signal stability properties for the dynamic RC network model (12). We perform a nonlinear analysis in the spirit of Brayton-Moser [25], [26], [124], [83], [85] and adapt the energy function (38) towards a *potential function*‡ accounting for resistive power losses and power dissipation by the (constant impedance, constant current, and constant power) loads as

$$\mathcal{W}(V) = \frac{1}{2}V^\mathsf{T}(\mathcal{L}_R + G)V - \mathbf{ln}(V)^\mathsf{T}P^* - V^\mathsf{T}I^*\,,$$

where $\mathbf{ln}V = (\ln V_1, \ldots, \ln V_n)^\mathsf{T}$. A straightforward calculation then shows that the RC network model (12) reads as

$$C\dot{V} = -\nabla\mathcal{W}(V)\,,$$

meaning that the potentials V evolve according to the gradient of the power-like function $\mathcal{W}(V)$. Critical points of the function $\mathcal{W}(V)$ are therefore equilibrium points of (12), and vice-versa. It follows by standard results for gradient systems that all bounded trajectories of (12) converge to equilibrium points [146, Chapter 15]. By requiring the Hessian of $\mathcal{W}(V)$ to be positive definite, one can show strict convexity of $\mathcal{W}(V)$ and that the equilibrium specified by Proposition 6.1 is locally asymptotically stable, which recovers the result of Proposition 6.3. An estimate of the region of attraction of V^* can be obtained by finding a compact sublevel set of $\mathcal{W}(V)$ containing V^*. We refer to [112], [32], [42] for related stability analyses of DC networks, to [35], [105] for a comprehensive survey concerning energy functions in AC power systems, and to [84], [104], [135] for further reading on power and energy-based approaches to nonlinear networks.

B. AC circuits and power networks

This section examines the important case where, in steady-state, all current sources and all internal voltages and currents in the RLC network (11) are harmonic with synchronous alternating current (AC) angular frequency ω:

$$I_i^*(t) = \sqrt{2}\,|I_i^*|\cos(\omega t + \phi_i)\,, \tag{51a}$$
$$V_i(t) = \sqrt{2}\,|V_i|\cos(\omega t + \theta_i)\,, \tag{51b}$$
$$f_i(t) = \sqrt{2}\,|f_i|\cos(\omega t + \varphi_i)\,. \tag{51c}$$

‡We remark that the considered RC circuit (12) is a simple yet illustrative subcase within the general Brayton-Moser modeling and analysis framework that can also account for inductive dynamics and more general nonlinearities.

Here $|I_i^*|, |V_i|, |f_i| \geq 0$ are the constant steady-state root-mean-square amplitudes of the waveforms, and $\phi_i, \theta_i, \varphi_i$ are the respective phase shifts. The RLC network (11) exhibits such steady-state solutions $(V(t), f(t))$ whenever the dynamics are internally stable and the injections I^* are as in (51a).

Unlike DC power, AC power is typically transmitted in a three-phase configuration in which three wires (plus a neutral wire) are used. Therefore, for each node (resp. edge) there are three potential and current injection (resp. voltage drop and current flow) waveforms to consider. When such a three-phase circuit is *balanced*, the harmonic waveforms on the three wires are separated by $\pm 120°$, and a standard equivalent circuit technique allows the three-phase circuit to be studied in terms of a single-phase equivalent circuit [73, Chapter 1]. We therefore proceed with a single-phase analysis in this section, with the understanding that the results can quickly be applied to balanced three-phase AC circuits.

1) Phasor analysis of AC circuits: We may equivalently express the harmonic signals in (51) as the real parts of complex-valued signals

$$I_i^*(t) = \Re\big(\underbrace{\sqrt{2}\,|I_i^*|e^{\mathrm{j}\phi_i}}_{\mathcal{I}_i^*\in\mathbb{C}}\,e^{\mathrm{j}\omega t}\big)\,,\quad V_i(t) = \Re\big(\underbrace{\sqrt{2}\,|V_i|e^{\mathrm{j}\theta_i}}_{\mathcal{V}_i\in\mathbb{C}}\,e^{\mathrm{j}\omega t}\big),$$
$$f_i(t) = \Re\big(\underbrace{\sqrt{2}\,|f_i|e^{\mathrm{j}\varphi_i}}_{\mathcal{F}_i\in\mathbb{C}}\,e^{\mathrm{j}\omega t}\big). \tag{52}$$

The complex quantities in brackets are referred to as a *phasors*, with $\mathcal{I}_i^*, \mathcal{V}_i$ and $\mathcal{F}_i$ being the complex "amplitudes" of the phasors. The classic approach to study AC electrical networks is to represent all potentials and current flows using phasors, and subsequently derive algebraic equations relating the vectors of complex amplitudes $\mathcal{V}, \mathcal{F}$, and $\mathcal{I}^*$. With this phasor substitution, the RLC circuit equations (11) reduce to the set of complex-valued algebraic equations§

$$\mathrm{j}\omega C\mathcal{V} = -G\mathcal{V} - B\mathcal{F} + \mathcal{I}^*, \tag{53a}$$
$$\mathrm{j}\omega L\mathcal{F} = B^\mathsf{T}\mathcal{V} - R\mathcal{F}\,, \tag{53b}$$

where $\mathcal{V}, \mathcal{F}, \mathcal{I}^*$ are the vectors of phasor amplitudes for potentials, edge currents, and constant-current injections, respectively. Solving (53b) for $\mathcal{F} = (R + \mathrm{j}\omega L)^{-1}B^\mathsf{T}\mathcal{V}$ and eliminating $\mathcal{F}$ from (53a), the electrical network is compactly described by the algebraic equation

$$\mathcal{I}^* = Y\mathcal{V} = \Big(\underbrace{B(R + \mathrm{j}\omega L)^{-1}B^\mathsf{T}}_{\text{complex-weighted network}} + \underbrace{(G + \mathrm{j}\omega C)}_{\text{complex shunts}}\Big)\mathcal{V}\,. \tag{54}$$

The so-called *admittance matrix* $Y \in \mathbb{C}^{n\times n}$ is a sum of two terms, the first being a Laplacian matrix $\mathcal{L}_{R+\mathrm{j}\omega L} = B(R + \mathrm{j}\omega L)^{-1}B^\mathsf{T}$ with complex weights $\frac{1}{r_{ij}+\mathrm{j}\omega\ell_{ij}}$ termed *admittances*. The second term in (54) is a complex diagonal matrix modeling the shunt admittance elements connected to ground at each node. The linear equation (54) is exactly analogous to the linear resistive circuit equation (13) studied in Section V-A, with analogous solution $\mathcal{V} = Y^{-1}\mathcal{I}^*$, and the corresponding real harmonic signals are recovered via (52).

§Constant power loads are omitted, and will be treated independently in our subsequent discussion of AC power flow.

While the static resistive circuit solution of Section V-A generalizes to the present AC case (54), many questions concerning effective resistance and Kron reduction for complex-weighted graphs remain unresolved; see [52].

2) Instantaneous power, complex power, and power flow equations: Often in AC circuit analysis — and in particular, in the study of power systems — one is interested in specifying the sources and loads of a circuit in terms of power and voltage, rather than current and voltage. For example, the energy production of a synchronous generator is scheduled in terms of power and not current, since power is more directly related to engineering specifications and monetary cost. To move towards such a power-focused formulation of the circuit equations, define the *instantaneous power* $p_i(t)$ injected into node $i \in \{1, \dots, n\}$ as $p_i(t) = V_i(t) I_i^*(t)$. Using the harmonic representations (51), some simple trigonometry shows that

$$\begin{aligned} p_i(t) = |V_i||I_i^*| \cos(\theta_i - \phi_i)\big(1 + \cos(2(\omega t + \theta_i))\big) \\ + |V_i||I_i^*| \sin(\theta_i - \phi_i) \sin(2(\omega t + \theta_i)). \end{aligned}$$

The instantaneous power consists of two oscillatory terms, only the first of which has non-zero mean. The *average* (also called *active* or *real*) power injected into node i over one cycle is defined as this mean component of the first term:

$$P_i = \frac{1}{T} \int_0^T p_i(t)\,\mathrm{d}t = |V_i||I_i^*| \cos(\theta_i - \phi_i)\,,$$

where $T = 2\pi/\omega$. Note that the active power P_i is zero if potential and current waveforms are 90° out of phase: $|\theta_i - \phi_i| = \pi/2$. The second oscillatory term in $p_i(t)$ has zero mean, but its amplitude

$$Q_i = |V_i||I_i^*| \sin(\theta_i - \phi_i)$$

is commonly referred to as *reactive* (or *imaginary*) power [1]. Reactive power reflects the zero-average energy exchange between inductive or capacitive elements, with power flowing into the element for half an AC cycle and out of the element during the remaining half (cf., the circulating power in (39)).¶

Again, it is most convenient to study power in AC circuits using phasors. To develop a phasor representation, define the *complex power* $S_i = P_i + \mathrm{j}Q_i \in \mathbb{C}$ injected at node $i \in \{1, \dots, n\}$ using the voltage and current phasors $\mathcal{V}_i$ and $\mathcal{I}_i^*$ as

$$S_i = \frac{1}{2} \mathcal{V}_i \overline{\mathcal{I}}_i^*\,.$$

where $\overline{\mathcal{I}}_i^*$ is the complex conjugate of $\mathcal{I}_i^*$. We have through simple calculations then that

$$S_i = \underbrace{|V_i||I_i^*| \cos(\theta_i - \phi_i)}_{=P_i} + \mathrm{j} \underbrace{|V_i||I_i^*| \sin(\theta_i - \phi_i)}_{=Q_i}\,.$$

The real part of S_i is exactly the real power P_i, while the imaginary part Q_i is the reactive power. In vector notation, the complex power is given by

$$S = P + \mathrm{j}Q = \frac{1}{2} \mathcal{V} \odot \overline{\mathcal{I}^*} = \frac{1}{2} \mathcal{V} \odot (\overline{Y\mathcal{V}}),$$

where we have inserted (54) to eliminate $\mathcal{I}^*$. Expanding the right-hand side and separating real and imaginary parts, we arrive at the *AC power flow equations* [90]

$$P_i = \sum_{j=1}^n |V_i||V_j| \left(\Re(Y_{ij}) \cos(\theta_i - \theta_j) + \Im(Y_{ij}) \sin(\theta_i - \theta_j)\right),$$

$$Q_i = \sum_{j=1}^n |V_i||V_j| \left(\Re(Y_{ij}) \sin(\theta_i - \theta_j) - \Im(Y_{ij}) \cos(\theta_i - \theta_j)\right),$$

for $i \in \{1, \dots, n\}$. These nonlinear equations relate the active and reactive power injections P_i and Q_i at each node to the complex voltage variables $|V_i| e^{\mathrm{j}\theta_i}$ at the neighboring nodes.

The power flow equations are highly nonlinear; in Section VI-B3 we examine this nonlinearity in some detail. Quick insight however can be gained by studying their linearization around $\theta = \mathbb{0}_n$ and $|V| = \mathbb{1}_n$, which is given by [20]

$$\begin{bmatrix} P \\ Q \end{bmatrix} \approx \begin{bmatrix} \Im(Y) & -\Re(Y) \\ -\Re(Y) & -\Im(Y) \end{bmatrix} \begin{bmatrix} \theta \\ |V| \end{bmatrix}. \tag{55}$$

Each subblock of the block matrix in (55) is a Laplacian (or negative Laplacian) matrix, possibly with additional diagonal elements in each subblock. Note that $\Re(Y)$ arises from the resistive component of the interconnection between nodes, while $\Im(Y)$ arises from inductances. In other words, when written in this form, a multigraph structure naturally appears. To our knowledge, the algebraic and spectral properties of the matrix in (55) are not well understood, and an analysis of (55) in the spirit of that from Section V-A remains open.

3) AC power flow problems: The AC power flow equations are the heart of almost all power system analysis, operations, optimization, and control. The analytic study of these equations dates back at least fifty years; we do not attempt to present a comprehensive overview of the area, but will present a selection of results based on the authors' experiences. We refer the reader to [118], [119] for a recent literature review.

In an *AC power flow problem*, a subset of the variables $\{|V_i|, \theta_i, P_i, Q_i\}$ are specified at a subset of nodes, and the problem is to solve the nonlinear AC power flow equations to determine the remaining unspecified variables. This is directly analogous to the problem of solving a static resistive circuit as in Section V-A, or the problem of determining an equilibrium point for a nonlinear circuit as in Section VI-A. As a specific instance of an AC power flow problem, we examine the case of a purely inductive interconnection with L positive definite and $R = \mathbb{0}$, with no shunt conductances $G = \mathbb{0}$ and no shunt capacitances $C = \mathbb{0}$. The important feature here is the lack of resistive elements; the network transfers power without resistive power losses. This instance is complex enough to highlight the important role of algebraic graph theory concepts, but simple enough to actually permit some insightful analysis.

The formal modeling for a power flow problem proceeds as follows. We begin with an undirected, connected and weighted graph $\mathcal{G}$. The nodes $\{1, \dots, n\}$ of the graph are partitioned into two subsets: a non-empty subset $\mathsf{PV} \subseteq \{1, \dots, n\}$ and a disjoint strict subset $\mathsf{PQ} \subset \{1, \dots, n\}$ such that $\{1, \dots, n\} = \mathsf{PQ} \cup \mathsf{PV}$. At node $i \in \mathsf{PV}$, the average power injection P_i and the RMS potential $|V_i|$ are specified; in power systems,

¶We remark that when a circuit does not a reach a sinusoidal steady state, e.g., in presence of nonlinear elements, then the definition and interpretation of reactive power is still a controversial and contested subject [82].

such a node corresponds to a generator with a scheduled power production P_i and a voltage level $|V_i|$ regulated by a local controller. At node $i \in \mathsf{PQ}$, the real power P_i and reactive power Q_i are specified; this corresponds to a constant power injection/demand, modeling a load or converter-interfaced renewable energy source. In networks with non-zero edge resistances or non-zero shunt conductances, one generally requires the presence of a third node type called a slack node, where θ_i and $|V_i|$ are specified with P_i and Q_i undetermined. The primary purpose of this node is to compensate for the resistive power dissipation in the network by supplying additional power. We will restrict our attention to lossless systems and will therefore omit the slack bus.

Given the above specified quantities, the AC power flow problem is to determine the phase angles θ_i for $i \in \mathsf{PQ} \cup \mathsf{PV}$ and the RMS potentials $|V_i|$ for $i \in \mathsf{PQ}$.

Under these modelling assumptions, the admittance matrix becomes purely imaginary and reduces to $Y = -\mathrm{j}B(\omega L)^{-1}B^{\mathsf{T}} = -\mathrm{j}\mathcal{L}_{\omega L}$. The power flow equations simplify to

$$P_i = \sum_{j=1}^{n} |V_i||V_j|\Im(Y_{ij})\sin(\theta_i - \theta_j)\,, \quad i \in \mathsf{PQ} \cup \mathsf{PV}, \tag{56a}$$

$$Q_i = -\sum_{j=1}^{n} |V_i||V_j|\Im(Y_{ij})\cos(\theta_i - \theta_j)\,, i \in \mathsf{PQ}\,. \tag{56b}$$

If the equations (56) can be solved for the PV/PQ node phase angles θ_i and the PQ bus potentials $|V_i|$, the remaining unspecified reactive power injections Q_i for $i \in \mathsf{PV}$ are uniquely determined by back substitution. An immediate insight is obtained from (56a) by summing over all $i \in \mathsf{PQ} \cup \mathsf{PV}$ and using the fact that $\sin(\cdot)$ is odd, from which we find that

$$\sum\nolimits_{i=1}^{n} P_i = 0 \qquad \Longleftrightarrow \qquad P \in \mathbb{1}_n^{\perp}\,.$$

This simply says that in such a lossless network, the real power generation must always be balanced by the real power demand.

An analysis of the lossless power flow problem (56) is possible, but becomes notationally quite involved and uses some additional graph-theoretic constructions that go beyond the scope of this survey; we refer the reader to [118], [119] for a detailed analysis. To study a comparatively tractable scenario, consider the case where $\mathsf{PQ} = \emptyset$; this specific model arises in the study of dynamic stability in a network of synchronous generators [51]. In this case, the products $k_{ij} = |V_i||V_j|\Im(Y_{ij})$ are constants, and (56) simplifies to

$$P_i = \sum\nolimits_{j=1}^{n} k_{ij}\sin(\theta_i - \theta_j)\,, \quad i \in \{1, \dots, n\}\,, \tag{57}$$

or in vectorized notation

$$P = B\mathcal{K}\,\mathbf{sin}(B^{\mathsf{T}}\theta)\,, \tag{58}$$

where $\mathcal{K} = \operatorname{diag}(\{k_e\}_{e \in \{1,\dots,m\}})$ and $\mathbf{sin}(x) = (\sin(x_1), \dots, \sin(x_n))^{\mathsf{T}}$. The network topology clearly affects the solvability of (58) through the incidence matrix B. In fact, linearizing the equation (58) around $\theta = \mathbb{0}_n$, we find that

$$P \approx B\mathcal{K}B^{\mathsf{T}}\theta = \mathcal{L}_{\mathcal{K}}\theta, \tag{59}$$

which is a linear Laplacian equation analogous to (13). To further emphasize the role of the topology, we can rewrite (58) as the two coupled equations

$$P = B\mathcal{K}\psi\,, \tag{60a}$$

$$\psi = \mathbf{sin}(B^{\mathsf{T}}\theta)\,, \tag{60b}$$

where $\psi \in \mathbb{R}^m$ is an auxiliary vector of variables. Some immediate insights can be gained by comparing (60) to the KCL and KVL equations (7) and (9) from Section IV-A. The first equation (60a) corresponds to the KCL equation (7), with current injections $I = P$ and current flows $f = \mathcal{K}\psi$. A comparison of (60b) and (9) shows that (60b) is a type of nonlinear KVL equation with potentials θ and voltage drops ψ. The combined equation (60) is directly analogous to the resistive network nodal current balance equation (18).

In practice we are interested in solutions of (60) for which the differences between phase angles of neighboring buses are relatively small. To quantify this, for $\gamma \in [0, \frac{\pi}{2})$, define

$$\Delta(\gamma) = \{\theta \in \mathbb{T}^n \mid |\theta_i - \theta_j| \leq \gamma \text{ for } \{i,j\} \in \mathcal{E}\}$$

as the subset of $\mathbb{T}^n$ (the n-torus) where phase angle differences along edges $\{i,j\} \in \mathcal{E}$ are less than γ.

Proposition 6.4 (PV node power flow problem [54], [80]): Consider the PV node power flow problem (57) with $P \in \mathbb{1}_n^{\perp}$, and let $\gamma \in [0, \pi/2)$. The following statements hold:

(i) Every solution of (60a) is of the form

$$\psi_{\text{general}} = B^{\mathsf{T}}\mathcal{L}_{\mathcal{K}}^{\dagger}P + \psi_{\text{hom}}\,, \tag{61}$$

where $\mathcal{L}_{\mathcal{K}} = B\mathcal{K}B^{\mathsf{T}}$ and $\mathcal{K}\psi_{\text{hom}} \in \operatorname{Ker}(B)$;

(ii) there exists a solution $\theta^* \in \Delta(\gamma)$ if and only if there exists ψ_{hom} such that $\|\psi_{\text{general}}\|_\infty \leq \sin(\gamma)$ and $\mathbf{arcsin}(\psi_{\text{general}}) \in \operatorname{Im}(B^{\mathsf{T}})$ (modulo 2π);

(iii) for graphs $\mathcal{G}$ containing no cycles, there exists a unique solution $\theta^* \in \Delta(\gamma)$ if and only if

$$\|B^{\mathsf{T}}\mathcal{L}_{\mathcal{K}}^{\dagger}P\|_\infty \leq \sin(\gamma)\,; \tag{62}$$

(iv) there exists a unique solution $\theta^* \in \Delta(\gamma)$ if

$$\|B^{\mathsf{T}}\mathcal{L}_{\mathcal{K}}^{\dagger}P\|_2 \leq \sin(\gamma)\,. \tag{63}$$

Equation (61) shows that every solution of the KCL-like equation (60a) can be decomposed into two terms: a particular solution belonging to the cutset space $\operatorname{Im}(B^{\mathsf{T}})$, and a homogeneous component belonging to the weighted cycle space $\mathcal{K}^{-1}\operatorname{Ker}(B)$. In fact, the particular solution $B^{\mathsf{T}}\mathcal{L}_{\mathcal{K}}^{\dagger}P$ is exactly the edge-wise phase differences one would calculate by solving the linearized equation (59). Item (ii) of Proposition 6.4 connects this linear solution to the full nonlinear equation (58) by requiring that ψ_{general} satisfies a boundedness condition $\|\psi_{\text{general}}\|_\infty \leq \sin(\gamma)$ along with the *cycle constraints* $\mathbf{arcsin}(\psi_{\text{general}}) \in \operatorname{Im}(B^{\mathsf{T}})$ (modulo 2π); the latter ensures that phase angle differences add up to a multiple of 2π around any undirected cycle of the graph (cf. KVL (5)). In graphs without cycles (item (iii)) the cycle constraints can be discarded, and the existence of a solution is equivalent to satisfaction of the boundedness condition. The analysis of (60) becomes considerably more challenging in networks with cycles, and only conservative sufficient conditions ensuring existence are known; we refer to [54], [53], [44], [45] for details and recent results. Specifically, the sufficient condition (iv) and a generalized version of fact (iii) are proved in [80].

At this point in our discussion of AC power flow we have reached the research frontier concerning graph-theoretic insights and analytic approaches to the solution space of the AC power flow equations. The development of graph-theoretic conditions for the existence and uniqueness of AC power flow solutions (and stability conditions for associated power system dynamics, which we have not discussed here) remains an area of active research. Among many recent works, we refer to [121], [58], [57], [22], [118], [119], [141], [59].

VII. Conclusions and Avenues for Future Research

The field of algebraic graph theory has been initially developed, amongst others, by electrical engineers to abstract and facilitate the study of electrical networks. Conversely, several fundamental concepts in algebraic graph theory were born out of concrete circuit problems. In this article, we highlighted the rich interplay between these two disciplines in the static and dynamic, linear and nonlinear, and real-valued and complex-valued cases. We reviewed classical results from the early days of network analysis as well as recent results. Our developments were centered around a single yet rich prototypical model of an electrical network.

The literature on the topic of this article is vast and mature. We hope to have delivered a survey and a tutorial exposition, as seen from the perspective of algebraic graph theory, that brought the reader from the basics all the way to the research frontier. We want to conclude by listing a few fundamental open problems at the intersection of electrical networks and algebraic graph theory. The list is by no means complete and is colored by our own interests and experiences.

In this paper we have studied networks in which each constitutive element is a one-port, described by a single voltage-current relationship between its terminals. More generally, electric elements such as transformers and gyrators require the adoption of 2-port representations. A future research direction is to adopt algebraic graph theory to model and study two-port networks. Along the same lines, much of the presented theory still has to be extended to circuit elements with nonlinear constitutive relations such as diodes and transistors.

We have shown that AC networks give rise to complex-valued graph matrices. In general, many of the results we presented for real-valued Laplacian (and more general Metzler) matrices have few (or no) complex-valued counterparts. Yet the study of complex-valued matrices and their associated graphs is of the utmost importance for large-scale AC power system applications. Another frontier in this regard are hybrid DC/AC networks and unbalanced multi-phase networks.

At the intersection of nonlinear and AC networks lie the celebrated power flow equations. The characterization of solutions to these equations, as a function of the network parameters and topology, has a long history and has witnessed some exciting recent developments. Yet in the full nonlinear and lossy setting, the basic existence and uniqueness questions are still unresolved, and the study of dynamics in such networks is a wide open field that is currently seeing much activity. With regards to our prototypical model (11), we performed a thorough linear analysis of the dynamics, though a full nonlinear large-signal stability analysis is still open.

Finally, a topic of historic interest was to reverse the reduction of electrical networks [12], [68], [137], [8], e.g., by embedding a cyclic network into a higher-dimensional equivalent acyclic network as in Figure 6. Since many circuit and power flow problems are analytically and computationally tractable only in acyclic networks, it would be of interest to find more general high-dimensional network embeddings and equivalence transformations. Likewise, the passive network synthesis problem [24] has recently received a revived interest and triggered many open questions [78].

Appendix

A. Compartmental systems

In this appendix we present a self-contained concise treatment of compartmental systems. For more complete treatments and proofs of the following statements we refer to [140], [79] and [27, Chapter 9].

A *compartmental system* is a dynamical system in which material is stored at storage nodes, called *compartments*, and is transferred along the edges of directed graph, called the *compartmental digraph*; see Figure 18(b). Each compartment

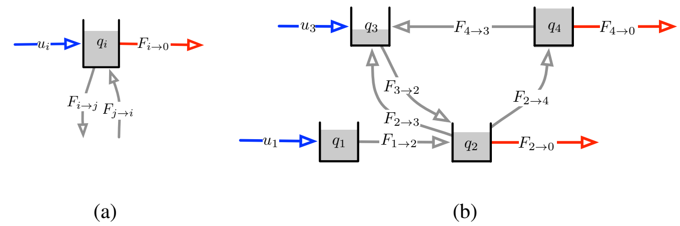

Fig. 18. (a) A compartment with inflow u_i, outflow $F_{i\to 0}$, and inter-compartmental flows $F_{i\to j}$. (b) A compartmental system with two inflows and two outflows; images courtesy of [27].

contains a time-varying quantity $q_i(t)$ and each directed arc (i,j) represents a *mass flow*, denoted $F_{i\to j}$, from compartment i to compartment j. The inflow from the environment into compartment i is denoted by u_i and the outflow from compartment i into the environment is denoted by $F_{i\to 0}$.

In a *linear compartmental system,* we assume

$$\begin{aligned} F_{i\to j}(q,t) &= f_{ij} q_i, && \text{for } j \in \{1,\dots,n\}, \\ F_{i\to 0}(q,t) &= f_{0i} q_i, && \text{and} \quad u_i(q,t) = u_i. \end{aligned}$$

for appropriate flow rate coefficients. More precisely, a *linear compartmental system* consists of

(i) a nonnegative $n \times n$ matrix $F = (f_{ij})_{i,j\in\{1,\dots,n\}}$ with zero diagonal, called the *flow rate matrix*,
(ii) a vector $f_0 \geq \mathbb{0}_n$, called the *outflow rates vector*, and
(iii) a vector $u \geq \mathbb{0}_n$, called the *inflow vector*.

The flow rate matrix F is the adjacency matrix of the compartmental digraph $\mathcal{G}_F$ (a weighted digraph without self-loops).

The *instantaneous flow balance* provides the affine dynamics of the system:

$$\dot{q}_i(t) = -\Big(f_{0i} + \sum_{j=1, j\neq i}^{n} f_{ij}\Big) q_i(t) + \sum_{j=1, j\neq i}^{n} f_{ji} q_j(t) + u_i.$$

The *compartmental matrix* $C = (c_{ij})_{i,j\in\{1,\dots,n\}}$ of a linear compartmental system is a Metzler matrix defined by

$$c_{ij} = \begin{cases} f_{ji}, & \text{if } i \neq j, \\ -f_{0i} - \sum_{h=1,h\neq i}^{n} f_{ih}, & \text{if } i = j. \end{cases}$$

Equivalently, $C = F^\top - \mathrm{diag}(F\mathbb{1}_n + f_0)$ and $\dot{q}(t) = Cq(t) + u$.

In the compartmental digraph, a set of compartments S is *outflow-connected* if there exists a directed path from every compartment in S to the environment, that is, to a compartment j with a positive flow rate constant $f_{0j} > 0$. Moreover a set of compartments S is *inflow-connected* if there exists a directed path from the environment to every compartment in S, that is, from a compartment i with a positive inflow $u_i > 0$.

Recall that, given a digraph $\mathcal{G}$, its *condensation* is a digraph whose nodes are the strongly connected components of $\mathcal{G}$ and whose edges are defined by corresponding edges in $\mathcal{G}$.

With these definitions, the following graph-theoretical and algebraic statements are known to be equivalent:

(i) the system is outflow-connected,
(ii) each sink (node without outgoing edges) of the condensation of $\mathcal{G}_F$ is outflow-connected, and
(iii) the compartmental matrix C is Hurwitz.

Theorem A.1 (Asymptotic behavior of compartmental systems): Consider a linear compartmental system (F, f_0, u) with compartmental matrix C and compartmental digraph $\mathcal{G}_F$. If the system is outflow-connected, then

(i) the compartmental matrix C is invertible,
(ii) every solution tends exponentially to the unique equilibrium $q^* = -C^{-1}u \geq \mathbb{0}_n$, and
(iii) in the ith compartment $q_i^* > 0$ if and only if the ith compartment is inflow-connected to a positive inflow.

B. *Proof of Lemma 5.13: Spectrum of the saddle matrix*

The following proof adopts elements from [34], [50], [49].

Regarding the first statement 1), we resort to a Lyapunov-based proof. Consider the auxiliary linear dynamical system

$$\begin{bmatrix}\dot{x}_1 \\ \dot{x}_2\end{bmatrix} = \begin{bmatrix}-G & -B \\ B^\top & -R\end{bmatrix}\begin{bmatrix}x_1 \\ x_2\end{bmatrix} = \mathcal{A}\begin{bmatrix}x_1 \\ x_2\end{bmatrix}, \tag{64}$$

and the Lyapunov function $\mathcal{V}(x_1, x_2) = \frac{1}{2}\|x_1\|^2 + \frac{1}{2}\|x_2\|^2$. The derivative of $\mathcal{V}(x, y)$ is given by

$$\dot{\mathcal{V}}(x_1, x_2) = -x_1^\top G x_1 - x_2^\top R x_2 \leq 0\,.$$

It follows that the state (x_1, x_2) is bounded. Thus, the matrix $\mathcal{A}$ admits only eigenvalues with strictly negative real part or eigenvalues on the imaginary axis with equal algebraic and geometric multiplicity.

Statement 2) is a corollary of Proposition 5.12.

If G and R are positive definite, then $\dot{\mathcal{V}}(x_1, x_2)$ is negative definite. It follows that the dynamics (64) are asymptotically stable and $\mathcal{A}$ is Hurwitz. This proves the third statement 3).

Regarding the fourth statement 4): To prove the first part, we follow the proof method of [34, Lemma 5.3]. Recall from statement 1) that the spectrum of $\mathcal{A}$ is restricted to the closed left half-plane. We aim to prove that, under the stated assumptions, no imaginary eigenvalues other than zero can occur. We reason by contradiction. Let $\mathrm{j}\sigma$, with $\sigma \neq 0$, be an imaginary eigenvalue of $\mathcal{A}$ with corresponding non-zero eigenvector $x + \mathrm{j}y$, where $x = [x_1\ x_2]^\top, y = [y_1\ y_2]^\top \in \mathbb{R}^{n+m}$. Then the real and imaginary parts of the eigenvalue equation

$$\mathrm{j}\sigma(x + \mathrm{j}y) = \mathcal{A}(x + \mathrm{j}y) = \begin{bmatrix}-G & -B \\ B^\top & -R\end{bmatrix}\begin{bmatrix}x_1 + \mathrm{j}y_1 \\ x_2 + \mathrm{j}y_2\end{bmatrix}$$

yield the set of equations

$$-Gx_1 - Bx_2 = -\sigma y_1, \tag{65a}$$
$$-Gy_1 - By_2 = \sigma x_1, \tag{65b}$$
$$B^\top x_1 - Rx_2 = -\sigma y_2, \tag{65c}$$
$$B^\top y_1 - Ry_2 = \sigma x_2. \tag{65d}$$

We pre-multiply equation (65a), respectively (65c), by $x_1^\top$, respectively by $x_2^\top$, and arrive at $-x_1^\top G x_1 - x_1^\top B x_2 = -\sigma x_1^\top y_1$, respectively $x_2^\top B^\top x_1 - x_2^\top R x_2 = -\sigma x_2^\top y_2$. By adding these equations we get $-x_1^\top G x_1 - x_2^\top R x_2 = -\sigma(x_1^\top y_1 + x_2^\top y_2)$. Via analogous manipulations of equations (65b) and (65d), we obtain $-y_1^\top G y_1 - y_2^\top R y_2 = \sigma(x_1^\top y_1 + x_2^\top y_2)$. These two conditions imply that

$$\begin{bmatrix}x_1 \\ x_2\end{bmatrix}^\top \begin{bmatrix}G & \\ & R\end{bmatrix}\begin{bmatrix}x_1 \\ x_2\end{bmatrix} = -\begin{bmatrix}y_1 \\ y_2\end{bmatrix}^\top \begin{bmatrix}G & \\ & R\end{bmatrix}\begin{bmatrix}y_1 \\ y_2\end{bmatrix}.$$

Since G and R are positive semi-definite (possibly zero matrices) by assumption, we obtain $x_1 \in \ker(G)$, $y_1 \in \ker(G)$ and $x_2 \in \ker(R)$, $y_2 \in \ker(R)$. By further using $x_1 \in \ker(G)$, $y_1 \in \ker(G)$ in equations (65a) and (65b) we obtain $-Bx_2 = -\sigma y_1$ and $-By_2 = \sigma x_1$, that is, $x_1 \in \mathrm{Im}(B)$, $y_1 \in \mathrm{Im}(B)$. We have now established that both x_1 and y_1 belong to $\ker(G) \cap \mathrm{Im}(B)$ and therefore $x_1 = y_1 = \mathbb{0}_n$ by assumption. Similarly, we obtain $x_2 = y_2 = \mathbb{0}_m$. But it is a contraddiction to have $x + \mathrm{j}y$ equal to serve since it is an eigenvector.

Now we prove the second part of statement 4). If G is positive definite, the Schur determinant formula [160] yields

$$\det\left(\begin{bmatrix}-G & -B \\ B^\top & -R\end{bmatrix}\right) = \det(G)\cdot\det(R + B^\top G^{-1} B)\,.$$

Note that $\det(G) \neq 0$. If B has full rank m, i.e., the graph is acyclic (see statement (S1) in Section III), then $B^\top G^{-1} B$ has full rank, and $\det(R + B^\top G^{-1} B) \neq 0$. Due to these facts, the matrix $\mathcal{A}$ has no eigenvalue at zero and is thus Hurwitz.

The first part of the proof of statement 5) is analogous to that of statement 4). To prove the second part, we assume that R is positive definite and apply the Schur determinant formula:

$$\det\left(\begin{bmatrix}-G & -B \\ B^\top & -R\end{bmatrix}\right) = \det(R)\cdot\det(G + BR^{-1}B^\top)\,.$$

Note that $\det(R) \neq 0$ and $BR^{-1}B^\top = \mathcal{L}_R$ is a Laplacian matrix associated to a connected graph. If G has at least one diagonal element, then $\mathcal{L}_R + G$ is a nonsingular matrix, as discussed in Section III-7. Due to these facts, the matrix $\mathcal{A}$ has no eigenvalue at zero and is thus Hurwitz.

C. Proof of Proposition 6.2: Local stability of RLC network

Let (V^*, f^*) be the unique equilibrium point from Proposition 6.1, and consider the linearized dynamic model (50). Applying Proposition 5.13 item 5) to the saddle matrix $\mathcal{A}(V^*)$, we find that $\mathcal{A}(V^*)$ will be Hurwitz if

$$G_{ii} + \frac{P_i^*}{(V_i^*)^2} \geq 0\,, \qquad i \in \{1, \ldots, n\}\,,$$

with strict inequality for at least one value of $i \in \{1, \ldots, n\}$. By changing variables as $V_i^* = (V_{I^*})_i(1 + \delta_i)$, the above inequalities are equivalently reformulated as

$$g_i + \frac{P_i^*}{(V_{I^*})_i^2(1+\delta_i)^2} \geq 0\,, \qquad i \in \{1, \ldots, n\}\,,$$

again with strict inequality for at least one value of i. From the proof of Proposition 6.1, each component δ_i of the shifted potential variable δ satisfies $-\delta_{\max} \leq \delta_i \leq \delta_{\max}$, where $\delta_{\max}$ is given as in Proposition 6.1; the result follows by inserting the lower bound $-\delta_{\max}$ into the set of inequalities.

D. Proof of Proposition 6.3: Local stability of RC network

We proceed by linearizing the model (12) around the equilibrium point V^*. The Jacobian matrix of (12) is

$$J(V^*) := C^{-1} \underbrace{\left(-(\mathcal{L}_R + G) - \operatorname{diag}(P^*)\operatorname{diag}(V^*)^{-2}\right)}_{:=\mathcal{M}_1}\,.$$

Since C is diagonal and the matrix $\mathcal{M}_1$ is a symmetric Metzler matrix, it follows that $J(V^*)$ is Hurwitz if and only if $\mathcal{M}_1$ is negative definite. Substituting $V^* = \operatorname{diag}(V_{I^*})(\mathbb{1}_n + \delta^*)$ and defining the congruent matrix $\mathcal{M}_2 := \operatorname{diag}(V_{I^*})\mathcal{M}_1\operatorname{diag}(V_{I^*})/4$, it follows that $\mathcal{M}_1$ is negative definite if and only if

$$\mathcal{M}_2 = -P_{\mathrm{crit}} - \frac{1}{4}\operatorname{diag}(\mathbb{1}_n + \delta^*)^{-2}\operatorname{diag}(P^*)$$

is negative definite, where we have used the definition of P_{crit}. Since P_{crit} is symmetric and positive definite, by Sylvester's Inertia Theorem [30] $\mathcal{M}_2$ is negative definite if and only if

$$\mathcal{M}_3 := P_{\mathrm{crit}}^{-1}\mathcal{M}_2 = -I_n - \underbrace{\frac{1}{4}P_{\mathrm{crit}}^{-1}\operatorname{diag}(P^*)\operatorname{diag}(\mathbb{1}_n + \delta^*)^{-2}}_{:=\Delta}$$

is Hurwitz. Stability will now follow if $\rho(\Delta) < 1$. Since it always holds that $\rho(\Delta) \leq \|\Delta\|_\infty$, we compute that

$$\begin{aligned}\|\Delta\|_\infty &\leq \frac{1}{4}\|P_{\mathrm{crit}}^{-1}\operatorname{diag}(P^*)\|_\infty \|\operatorname{diag}(\mathbb{1}_n + \delta^*)^{-2}\|_\infty \\ &< \|P_{\mathrm{crit}}^{-1}\operatorname{diag}(P^*)\|_\infty < 1\,.\end{aligned}$$

where we have used the fact from Proposition 6.1 that $\delta_i^* \in (-\frac{1}{2}, \frac{1}{2})$ for each component i (in particular, we used the lower bound) and used (47). It follows that $\rho(\Delta) < 1$, and therefore that $J(V^*)$ is Hurwitz so V^* is locally exponentially stable.

References

[1] H. Akagi, E. H. Watanabe, and M. Aredes. *Instantaneous Power Theory and Applications to Power Conditioning*. John Wiley & Sons, 2017.

[2] M. Altmann. Reinterpreting network measures for models of disease transmission. *Social Networks*, 15(1):1–17, 1993. doi:10.1016/0378-8733(93)90019-H.

[3] C. S. Amin, M. H. Chowdhury, and Y. I. Ismail. Realizable reduction of interconnect circuits including self and mutual inductances. *IEEE Transactions on Computer-Aided Design of Integrated Circuits and Systems*, 24(2):271–277, 2005. doi:10.1109/TCAD.2004.840545.

[4] B. D. O. Anderson and S. Vongpanitlerd. *Network Analysis and Synthesis*. Dover, 2006.

[5] L. Aolaritei, S. Bolognani, and F. Dörfler. Hierarchical and distributed monitoring of voltage stability in distribution networks. *IEEE Transactions on Power Systems*, October 2017. Conditionally accepted. URL: https://arxiv.org/abs/1710.10544.

[6] G. I. Atabekov. *Linear Network Theory*. Pergamon Press, 1965.

[7] B. Bamieh, M. R. Jovanovic, P. Mitra, and S. Patterson. Coherence in large-scale networks: Dimension-dependent limitations of local feedback. *IEEE Transactions on Automatic Control*, 57(9):2235–2249, 2012. doi:10.1109/TAC.2012.2202052.

[8] V. V. Bapeswara Rao and V. K. Aatre. Mesh-star transformation. *Electronics Letters*, 10(6):73–74, 1974. doi:10.1049/el:19740056.

[9] N. Barabanov, R. Ortega, R. Grino, and B. Polyak. On existence and stability of equilibria of linear time-invariant systems with constant power loads. *IEEE Transactions on Circuits and Systems I: Fundamental Theory and Applications*, 63(1):114–121, 2016. doi:10.1109/TCSI.2015.2497559.

[10] P. Barooah and J. P. Hespanha. Estimation on graphs from relative measurements. *IEEE Control Systems*, 27(4):57–74, 2007. doi:10.1109/MCS.2007.384125.

[11] M. Bazrafshan and N. Gatsis. Convergence of the Z-bus method for three-phase distribution load-flow with ZIP loads. *IEEE Transactions on Power Systems*, 33(1):153–165, 2018. doi:10.1109/TPWRS.2017.2703835.

[12] S. Bedrosian. Converse of the star-mesh transformation. *IRE Transactions on Circuit Theory*, 8(4):491–493, 1961. doi:10.1109/TCT.1961.1086832.

[13] J. A. Belk, W. Inam, D. J. Perreault, and K. Turitsyn. Stability and control of ad hoc DC microgrids. In *IEEE Conf. on Decision and Control*, pages 3271–3278, Las Vegas, NV, USA, December 2016. doi:10.1109/CDC.2016.7798761.

[14] M. Benzi, G. H. Golub, and J. Liesen. Numerical solution of saddle point problems. *Acta Numerica*, 14:1–137, 2005. doi:10.1017/S0962492904000212.

[15] M. Benzi and N. Razouk. Decay bounds and $o(n)$ algorithms for approximating functions of sparse matrices. *Electronic Transactions on Numerical Analysis*, 28:16–39, 2007. URL: http://etna.mcs.kent.edu/vol.28.2007-2008/pp16-39.dir/pp16-39.pdf.

[16] N. Biggs. *Algebraic Graph Theory*. Cambridge University Press, 2 edition, 1994.

[17] N. Biggs. Algebraic potential theory on graphs. *Bulletin of the London Mathematical Society*, 29(6):641–682, 1997. doi:10.1112/S0024609397003305.

[18] D. A. Bini and B. Meini. The cyclic reduction algorithm: from Poisson equation to stochastic processes and beyond. *Numerical Algorithms*, 51(1):23–60, 2009. doi:10.1007/s11075-008-9253-0.

[19] B. Bollobás. *Modern Graph Theory*. Springer, 1998.

[20] S. Bolognani and F. Dörfler. Fast power system analysis via implicit linearization of the power flow manifold. In *Allerton Conf. on Communications, Control and Computing*, pages 402–409, Allerton, IL, USA, September 2015. doi:10.1109/ALLERTON.2015.7447032.

[21] S. Bolognani and S. Zampieri. A distributed control strategy for reactive power compensation in smart microgrids. *IEEE Transactions on Automatic Control*, 58(11):2818–2833, 2013. doi:10.1109/TAC.2013.2270317.

[22] S. Bolognani and S. Zampieri. On the existence and linear approximation of the power flow solution in power distribution networks. *IEEE Transactions on Power Systems*, 31(1):163–172, 2016. doi:10.1109/TPWRS.2015.2395452.

[23] L. Borcea, V. Druskin, and F. G. Vasquez. Electrical impedance tomography with resistor networks. *Inverse Problems*, 24(3):035013, 2008. doi:10.1088/0266-5611/24/3/035013.

[24] R. Bott and R. J. Duffin. Impedance synthesis without use of transformers. *Journal of Applied Physics*, 20(8):816–816, 1949. doi:10.1063/1.1698532.
[25] R. K. Brayton and J. K. Moser. A theory of nonlinear networks. I. *Quarterly of Applied Mathematics*, 22(1):1–33, 1964. doi:10.1090/qam/169746.
[26] R. K. Brayton and J. K. Moser. A theory of nonlinear networks. II. *Quarterly of Applied Mathematics*, 22(2):81–104, 1964. doi:10.1090/qam/169747.
[27] F. Bullo. *Lectures on Network Systems*. Version 0.96, January 2018. With contributions by J. Cortés, F. Dörfler, and S. Martínez. URL: http://motion.me.ucsb.edu/book-lns.
[28] S. Y. Caliskan and P. Tabuada. Towards Kron reduction of generalized electrical networks. *Automatica*, 50(10):2586–2590, 2014. doi:10.1016/j.automatica.2014.08.017.
[29] R. Carli, F. Garin, and S. Zampieri. Quadratic indices for the analysis of consensus algorithms. In *IEEE Information Theory and Applications Workshop*, pages 96–104, San Diego, CA, USA, February 2009. doi:10.1109/ITA.2009.5044929.
[30] D. Carlson and H. Schneider. Inertia theorems for matrices: The semidefinite case. *Journal of Mathematical Analysis and Applications*, 6:430–446, 1963.
[31] A. Carmona, A. M. Encinas, and M. Mitjana. Effective resistances for ladder-like chains. *International Journal of Quantum Chemistry*, 114(24):1670–1677, 2014. doi:10.1002/qua.24740.
[32] K. Cavanagh, J. A. Belk, and K. Turitsyn. Transient stability guarantees for ad hoc DC microgrids. *IEEE Control Systems Letters*, 2(1):139–144, 2018. doi:10.1109/LCSYS.2017.2764441.
[33] P. Chebotarev. Comments on "Consensus and cooperation in networked multi-agent systems". *Proceedings of the IEEE*, 98(7):1353–1354, 2010. doi:10.1109/JPROC.2010.2049911.
[34] A. Cherukuri, B. Gharesifard, and J. Cortes. Saddle-point dynamics: Conditions for asymptotic stability of saddle points. *SIAM Journal on Control and Optimization*, 55(1):486–511, 2017. doi:10.1137/15M1026924.
[35] H.-D. Chiang. *Direct Methods for Stability Analysis of Electric Power Systems*. John Wiley & Sons, 2011.
[36] L. O. Chua. *Introduction to Nonlinear Network Theory*. McGraw-Hill, 1969.
[37] L. O. Chua, C. A. Desoer, and E. S. Kuh. *Linear and Nonlinear Circuits*. McGraw-Hill, 1987.
[38] T. Coletta and P. Jacquod. Performance measures in electric power networks under line contingencies, 2017. URL: https://arxiv.org/abs/1711.10348.
[39] M. Colombino, D. Groß, and F. Dörfler. Global phase and voltage synchronization for power inverters: a decentralized consensus-inspired approach. In *IEEE Conf. on Decision and Control*, pages 5690–5695, Melbourne, Australia, December 2017. doi:10.1109/CDC.2017.8264518.
[40] E. Cotilla-Sanchez, P. D. H. Hines, C. Barrows, and S. Blumsack. Comparing the topological and electrical structure of the North American electric power infrastructure. *IEEE Systems Journal*, 6(4):616–626, 2012. doi:10.1109/JSYST.2012.2183033.
[41] E. B. Curtis and J. A. Morrow. *Inverse Problems for Electrical Networks*. World Scientific Publishing, 2000.
[42] C. De Persis, E. R. A. Weitenberg, and F. Dörfler. A power consensus algorithm for DC microgrids. *Automatica*, February 2017. Submitted. URL: https://arxiv.org/pdf/1611.04192.pdf.
[43] R. C. Degeneff, M. R. Gutierrez, S. J. Salon, D. W. Burow, and R. J. Nevins. Kron's reduction method applied to the time stepping finite element analysis of induction machines. *IEEE Transactions on Energy Conversion*, 10(4):669–674, 2002. doi:10.1109/60.475837.
[44] R. Delabays, T. Coletta, and P. Jacquod. Multistability of phase-locking and topological winding numbers in locally coupled Kuramoto models on single-loop networks. *Journal of Mathematical Physics*, 57(3):032701, 2016. doi:10.1063/1.4943296.
[45] R. Delabays, T. Coletta, and P. Jacquod. Multistability of phase-locking in equal-frequency Kuramoto models on planar graphs. *Journal of Mathematical Physics*, 58(3):032703, 2017. doi:10.1063/1.4978697.
[46] S. Demko, W. F. Moss, and P. W. Smith. Decay rates for inverses of band matrices. *Mathematics of Computation*, 43(168):491–499, 1984. URL: http://www.jstor.org/stable/2008290.
[47] S. V. Dhople, B. B. Johnson, F. Dörfler, and A. O. Hamadeh. Synchronization of nonlinear circuits in dynamic electrical networks with general topologies. *IEEE Transactions on Circuits and Systems I: Regular Papers*, 61(9):2677–2690, 2014. doi:10.1109/TCSI.2014.2332250.
[48] I. Dobson. Voltages across an area of a network. *IEEE Transactions on Power Systems*, 27(2):993–1002, 2011. doi:10.1109/TPWRS.2011.2168985.
[49] F. Dörfler. Lecture Notes on "Circuits & Power Grids", 2017. Part of the "Advanced Topics in Control" Course 2017. URL: http://control.ee.ethz.ch/~floriand/docs/Teaching/ATIC_2017/Circuits_Lecture.pdf.
[50] F. Dörfler. Lecture Notes on "Distributed Consensus-Based Optimization", 2017. Part of the "Advanced Topics in Control" Course 2017. URL: http://control.ee.ethz.ch/~floriand/docs/Teaching/ATIC_2017/Optimization_Lecture.pdf.
[51] F. Dörfler and F. Bullo. Synchronization and transient stability in power networks and non-uniform Kuramoto oscillators. *SIAM Journal on Control and Optimization*, 50(3):1616–1642, 2012. doi:10.1137/110851584.
[52] F. Dörfler and F. Bullo. Kron reduction of graphs with applications to electrical networks. *IEEE Transactions on Circuits and Systems I: Regular Papers*, 60(1):150–163, 2013. doi:10.1109/TCSI.2012.2215780.
[53] F. Dörfler and F. Bullo. Synchronization in complex networks of phase oscillators: A survey. *Automatica*, 50(6):1539–1564, 2014. doi:10.1016/j.automatica.2014.04.012.
[54] F. Dörfler, M. Chertkov, and F. Bullo. Synchronization in complex oscillator networks and smart grids. *Proceedings of the National Academy of Sciences*, 110(6):2005–2010, 2013. doi:10.1073/pnas.1212134110.
[55] P. G. Doyle and J. L. Snell. *Random Walks and Electric Networks*. Mathematical Association of America, 1984.
[56] K. Dvijotham and M. Chertkov. Convexity of structure preserving energy functions in power transmission: Novel results and applications. In *American Control Conference*, pages 5035–5042, 2015. doi:10.1109/ACC.2015.7172123.
[57] K. Dvijotham and M. Chertkov. Convexity of structure preserving energy functions in power transmission: Novel results and applications. In *American Control Conference*, pages 5035–5042, Chicago, USA, July 2015. doi:10.1109/ACC.2015.7172123.
[58] K. Dvijotham, M. Chertkov, and S. Low. A differential analysis of the power flow equations. In *IEEE Conf. on Decision and Control*, pages 23–30, Osaka, Japan, December 2015. doi:10.1109/CDC.2015.7402082.
[59] K. Dvijotham, E. Mallada, and J. W. Simpson-Porco. High-voltage solution in radial power networks: Existence, properties, and equivalent algorithms. *IEEE Control Systems Letters*, 1(2):322–327, 2017. doi:10.1109/LCSYS.2017.2717578.
[60] G. Escobar, A. J. van der Schaft, and R. Ortega. A Hamiltonian viewpoint in the modeling of switching power converters. *Automatica*, 35(3):445–452, 1999. doi:10.1016/S0005-1098(98)00196-4.
[61] F. Fagnani and P. Frasca. *Introduction to Averaging Dynamics over Networks*. Springer, 2017. doi:10.1007/978-3-319-68022-4.
[62] Y. Fan. Schur complements and its applications to symmetric nonnegative and Z-matrices. *Linear Algebra and its Applications*, 353(1-3):289–307, 2002. doi:10.1016/S0024-3795(02)00327-0.
[63] S. Fiaz, D. Zonetti, R. Ortega, J. M. A. Scherpen, and A. J. van der Schaft. A port-Hamiltonian approach to power network modeling and analysis. *European Journal of Control*, 19(6):477–485, 2013. doi:10.1016/j.ejcon.2013.09.002.
[64] M. Fiedler. Algebraic connectivity of graphs. *Czechoslovak Mathematical Journal*, 23(2):298–305, 1973. URL: http://dml.cz/dmlcz/101168.
[65] M. Fiedler. Inversion of bigraphs and connection with the Gaussian elimination. In *Graphs, Hypergraphs and Block Systems*, pages 57–68, Zielona Gora, Czechoslovakia, 1976.
[66] M. Fiedler. *Special Matrices and their Applications in Numerical Mathematics*. Martinus Nijhoff Publishers, 1986.
[67] S. Fortunato. Community detection in graphs. *Physics Reports*, 486(3-5):75–174, 2010. doi:10.1016/j.physrep.2009.11.002.
[68] R. Foster. An open question. *IRE Transactions on Circuit Theory*, 8(2):175–175, 1961. doi:10.1109/TCT.1961.1086780.
[69] F. Fouss, A. Pirotte, J. M. Renders, and M. Saerens. Random-walk computation of similarities between nodes of a graph with application to collaborative recommendation. *IEEE Transactions on Knowledge and Data Engineering*, 19(3):355–369, 2007. doi:10.1109/TKDE.2007.46.
[70] A. Ghosh, S. Boyd, and A. Saberi. Minimizing effective resistance of a graph. *SIAM Review*, 50(1):37–66, 2008. doi:10.1137/050645452.

[71] J. R. Gilbert. Predicting structure in sparse matrix computations. *SIAM Journal on Matrix Analysis and Applications*, 15(1):62–79, 1994. doi:10.1137/S0895479887139455.

[72] C. D. Godsil and G. F. Royle. *Algebraic Graph Theory*. Springer, 2001.

[73] A. Gómez-Expósito, A. J. Conejo, and C. Cañizares, editors. *Electric Energy Systems: Analysis and Operation*. CRC Press, 2017.

[74] D. Groß, C. Arghir, and F. Dörfler. On the steady-state behavior of a nonlinear power system model. *Automatica*, 90:248–254, 2018. doi:10.1016/j.automatica.2017.12.057.

[75] I. Gutman and W. Xiao. Generalized inverse of the Laplacian matrix and some applications. *Bulletin (Acadmie Serbe des Sciences et des Arts. Classe des sciences mathmatiques et naturelles. Sciences mathmatiques)*, 129(29):15–23, 2004. URL: http://emis.ams.org/journals/BSANU/29/2.html.

[76] H. Hao and P. Barooah. Asymmetric control achieves size-independent stability margin in 1-D flocks. In *IEEE Conf. on Decision and Control and European Control Conference*, pages 3458–3463, Orlando, FL, USA, December 2011. doi:10.1109/CDC.2011.6160339.

[77] B. D. Hughes. *Random Walks and Random Environments. Volume 1: Random Walks*. Clarendon Press, Oxford, 1995.

[78] T. H. Hughes and M. C. Smith. On the minimality and uniqueness of the Bott–Duffin realization procedure. *IEEE Transactions on Automatic Control*, 59(7):1858–1873, 2014. doi:10.1109/TAC.2014.2312471.

[79] J. A. Jacquez and C. P. Simon. Qualitative theory of compartmental systems. *SIAM Review*, 35(1):43–79, 1993. doi:10.1137/1035003.

[80] S. Jafarpour and F. Bullo. Synchronization of Kuramoto oscillators via cutset projections. *IEEE Transactions on Automatic Control*, November 2017. Submitted. URL: https://arxiv.org/abs/1711.03711.

[81] D. Janezic, A. Milicevic, S. Nikolic, and N. Trinajstic. *Graph-Theoretical Matrices in Chemistry*. CRC Press, 2015.

[82] D. Jeltsema. Budeanu's concept of reactive and distortion power revisited. In *International School on Nonsinusoidal Currents and Compensation*, pages 1–6, Lagow, Poland, June 2015. doi:10.1109/ISNCC.2015.7174697.

[83] D. Jeltsema, R. Ortega, and J. M. A. Scherpen. On passivity and power-balance inequalities of nonlinear RLC circuits. *IEEE Transactions on Circuits and Systems I: Fundamental Theory and Applications*, 50(9):1174–1179, 2003. doi:10.1109/TCSI.2003.816332.

[84] D. Jeltsema and J. M. A. Scherpen. A dual relation between port-Hamiltonian systems and the Brayton-Moser equations for nonlinear switched RLC circuits. *Automatica*, 39(6):969–979, 2003. doi:10.1016/S0005-1098(03)00070-0.

[85] D. Jeltsema and J. M. A. Scherpen. Multidomain modeling of nonlinear networks and systems. *IEEE Control Systems*, 29(4):28–59, 2009. doi:10.1109/MCS.2009.932927.

[86] A. E. Kennelly. The equivalence of triangles and three-pointed stars in conducting networks. *Electrical World and Engineer*, 34(12):413–414, 1899.

[87] Gustav Kirchhoff. Über die Auflösung der Gleichungen, auf welche man bei der Untersuchung der linearen Verteilung galvanischer Ströme geführt wird. *Annalen der Physik und Chemie*, 148(12):497–508, 1847. doi:10.1002/andp.18471481202.

[88] D. J. Klein and M. Randić. Resistance distance. *Journal of Mathematical Chemistry*, 12(1):81–95, 1993. doi:10.1007/BF01164627.

[89] G. Kron. *Tensor Analysis of Networks*. John Wiley & Sons, 1939.

[90] P. Kundur. *Power System Stability and Control*. McGraw-Hill, 1994.

[91] J. Lavei, A. Rantzer, and S. Low. Power flow optimization using positive quadratic programming. *IFAC Proceedings Volumes*, 44(1):10481–10486, 2011. 18th IFAC World Congress. doi:10.3182/20110828-6-IT-1002.02588.

[92] E. Lovisari, F. Garin, and S. Zampieri. Resistance-based performance analysis of the consensus algorithm over geometric graphs. *SIAM Journal on Control and Optimization*, 51(5):3918–3945, 2013. doi:10.1137/110857428.

[93] J. E. Machado, R. Gri, N. Barabanov, R. Ortega, and B. Polyak. On existence of equilibria of multi-port linear AC networks with constant-power loads. *IEEE Transactions on Circuits and Systems I: Regular Papers*, PP(99):1–11, 2017. doi:10.1109/TCSI.2017.2697906.

[94] J. Machowski, J. W. Bialek, and J. R. Bumby. *Power System Dynamics*. John Wiley & Sons, 2 edition, 2008.

[95] B. M. Maschke, A. J. van der Schaft, and P. C. Breedveld. An intrinsic Hamiltonian formulation of the dynamics of LC-circuits. *IEEE Transactions on Circuits and Systems*, 42(2):73–82, 1995. doi:10.1109/81.372847.

[96] B. H. McRae, B. G. Dickson, T. H. Keitt, and V. B. Shah. Using circuit theory to model connectivity in ecology, evolution, and conservation. *Ecology*, 89(10):2712–2724, 2008. doi:10.1890/07-1861.1.

[97] R. Merris. Laplacian matrices of a graph: A survey. *Linear Algebra and its Applications*, 197:143–176, 1994. doi:10.1016/j.laa.2011.11.0323374.

[98] C. D. Meyer. Stochastic complementation, uncoupling Markov chains, and the theory of nearly reducible systems. *SIAM Review*, 31(2):240–272, 1989. doi:10.1137/1031050.

[99] C. D. Meyer. *Matrix Analysis and Applied Linear Algebra*. SIAM, 2001.

[100] U. Miekkala. Graph properties for splitting with grounded Laplacian matrices. *BIT Numerical Mathematics*, 33(3):485–495, 1993. doi:10.1007/BF01990530.

[101] G. J. Minty. On the axiomatic foundations of the theories of directed linear graphs, electrical networks and network-programming. *Journal of Mathematics and Mechanics*, 15(3):485–520, 1966. URL: http://www.jstor.org/stable/24901346.

[102] B. Mohar. The Laplacian spectrum of graphs. In Y. Alavi, G. Chartrand, O. R. Oellermann, and A. J. Schwenk, editors, *Graph Theory, Combinatorics, and Applications*, volume 2, pages 871–898. John Wiley & Sons, 1991. URL: http://citeseerx.ist.psu.edu/viewdoc/summary?doi=10.1.1.96.2577.

[103] R. Olfati-Saber, J. A. Fax, and R. M. Murray. Consensus and cooperation in networked multi-agent systems. *Proceedings of the IEEE*, 95(1):215–233, 2007. doi:10.1109/JPROC.2006.887293.

[104] R. Ortega, A. J. van der Schaft, I. Mareels, and B. Maschke. Putting energy back in control. *IEEE Control Systems*, 21(2):18–33, 2001. doi:10.1109/37.915398.

[105] M. A. Pai. *Energy Function Analysis for Power System Stability*. Kluwer Academic Publishers, 1989.

[106] C. R. Paul. Modeling electromagnetic interference properties of printed circuit boards. *IBM Journal of Research and Development*, 33(1):33–50, 1989. doi:10.1147/rd.331.0033.

[107] J. H. H. Perk and H. Au-Yang. Yang-Baxter equations. In J.-P. Françoise, G. L. Naber, and S. T. Tsun, editors, *Encyclopedia of Mathematical Physics*, pages 465–473. Elsevier, 2006. doi:10.1016/B0-12-512666-2/00191-7.

[108] N. Perraudin, J. Paratte, D. Shuman, L. Martin, V. Kalofolias, P. Vandergheynst, and D. K. Hammond. GSPBOX: A toolbox for signal processing on graphs, August 2014. URL: https://arxiv.org/abs/1408.5781.

[109] M. Pirani and S. Sundaram. On the smallest eigenvalue of grounded Laplacian matrices. *IEEE Transactions on Automatic Control*, 61(2):509–514, 2016. doi:10.1109/TAC.2015.2444191.

[110] B. K. Poolla, S. Bolognani, and F. Dörfler. Optimal placement of virtual inertia in power grids. *IEEE Transactions on Automatic Control*, 62(12):6209–6220, 2017. doi:10.1109/TAC.2017.2703302.

[111] M. A. Porter, J.-P. Onnela, and P. J. Mucha. Communities in networks. *Notices of the AMS*, 56(9):1082–1097, 2009. URL: http://www.ams.org/notices/200909/rtx090901082p.pdf.

[112] A. Rantzer and B. Bernhardsson. Control of convex-monotone systems. In *IEEE Conf. on Decision and Control*, pages 2378–2383, Los Angeles, USA, December 2014. doi:10.1109/CDC.2014.7039751.

[113] J. Rommes and W. H. A. Schilders. Efficient methods for large resistor networks. *IEEE Transactions on Computer-Aided Design of Integrated Circuits and Systems*, 29(1):28–39, 2009. doi:10.1109/TCAD.2009.2034402.

[114] D. J. Rose, R. E. Tarjan, and G. S. Lueker. Algorithmic aspects of vertex elimination on graphs. *SIAM Journal on Computing*, 5(2):266–283, 1976. doi:10.1137/0205021.

[115] A. Rosen. A new network theorem. *Journal of the Institution of Electrical Engineers*, 62(335):916–918, 1924. doi:10.1049/jiee-1.1924.0120.

[116] W. Rudin. *Principles of Mathematical Analysis*. International Series in Pure and Applied Mathematics. McGraw-Hill, 3 edition, 1976.

[117] D. W. C. Shew. XXVII. generalized star and mesh transformations. *The London, Edinburgh, and Dublin Philosophical Magazine and Journal of Science*, 38(279):267–275, 1947. doi:10.1080/14786444708521594.

[118] J. W. Simpson-Porco. A theory of solvability for lossless power flow equations – Part I: Fixed-point power flow. *IEEE Transactions on Control of Network Systems*, 2017. To appear. doi:10.1109/TCNS.2017.2711433.

[119] J. W. Simpson-Porco. A theory of solvability for lossless power flow equations – Part II: Conditions for radial networks. *IEEE Transactions on Control of Network Systems*, 2017. To appear. doi:10.1109/TCNS.2017.2711859.

[120] J. W. Simpson-Porco, F. Dörfler, and F. Bullo. Synchronization and power sharing for droop-controlled inverters in islanded microgrids. *Automatica*, 49(9):2603–2611, 2013. doi:10.1016/j.automatica.2013.05.018.

[121] J. W. Simpson-Porco, F. Dörfler, and F. Bullo. Voltage collapse in complex power grids. *Nature Communications*, 7(10790), 2016. doi:10.1038/ncomms10790.

[122] J. W. Simpson-Porco, F. Dörfler, and F. Bullo. Voltage stabilization in microgrids via quadratic droop control. *IEEE Transactions on Automatic Control*, 62(7):1239–253, 2017. doi:10.1109/TAC.2016.2585094.

[123] J. W. Simpson-Porco and N. Monshizadeh. Model-free wide-area monitoring of power grids via cutset voltages. In *IEEE Conf. on Decision and Control*, pages 7508–7513, Las Vegas, NV, USA, December 2016. doi:10.1109/CDC.2016.7799429.

[124] S. Smale. On the mathematical foundations of electrical circuit theory. *Journal of Differential Geometry*, 7(1-2):193–210, 1972. doi:10.4310/jdg/1214430827.

[125] E. A. Stone and A. R. Griffing. On the Fiedler vectors of graphs that arise from trees by Schur complementation of the Laplacian. *Linear Algebra and its Applications*, 431(10):1869–1880, 2009. doi:10.1016/j.laa.2009.06.024.

[126] E. Tegling, B. Bamieh, and D. F. Gayme. The price of synchrony: Evaluating the resistive losses in synchronizing power networks. *IEEE Transactions on Control of Network Systems*, 2(3):254–266, 2015. doi:10.1109/TCNS.2015.2399193.

[127] B. D. H. Tellegen. A general network theorem, with applications. *Philips Research Reports*, 7(4):259–269, 1952.

[128] S. Trip, M. Bürger, and C. De Persis. An internal model approach to (optimal) frequency regulation in power grids with time-varying voltages. *Automatica*, 64:240–253, 2016. doi:10.1016/j.automatica.2015.11.021.

[129] M. Tucci, A. Floriduz, S. Riverso, and G. Ferrari-Trecate. Plug-and-play control of AC islanded microgrids with general topology. In *European Control Conference*, pages 1493–1500, June 2016. doi:10.1109/ECC.2016.7810501.

[130] M. Tyloo, T. Coletta, and P. Jacquod. Robustness of synchrony in complex networks and generalized Kirchhoff indices. *Physical Review Letters*, 2018. URL: https://arxiv.org/abs/1710.07536.

[131] A. J. van der Schaft. *L2-Gain and Passivity Techniques in Nonlinear Control*, volume 218 of *Lecture Notes in Control and Information Sciences*. Springer, 1996.

[132] A. J. van der Schaft. Characterization and partial synthesis of the behavior of resistive circuits at their terminals. *Systems & Control Letters*, 59(7):423–428, 2010. doi:10.1016/j.sysconle.2010.05.005.

[133] A. J. van der Schaft. Modeling of physical network systems. *Systems & Control Letters*, 2015. doi:10.1016/j.sysconle.2015.08.013.

[134] A. J. van der Schaft. The flow equations of linear resistive electrical networks, December 2017. URL: https://arxiv.org/abs/1712.10263.

[135] A. J. van der Schaft and B. M. Maschke. Port-Hamiltonian systems on graphs. *SIAM Journal on Control and Optimization*, 51(2):906–937, 2013. doi:10.1137/110840091.

[136] E. I. Verriest and J. C. Willems. The behavior of linear time invariant RLC circuits. In *IEEE Conf. on Decision and Control*, pages 7754–7758, Atlanta, GA, USA, December 2010. doi:10.1109/CDC.2010.5717364.

[137] L. Versfeld. Remarks on star-mesh transformation of electrical networks. *Electronics Letters*, 6(19):597–599, 1970. doi:10.1049/el:19700417.

[138] N. K. Vishnoi. $Lx = b$, Laplacian solvers and their algorithmic applications. *Theoretical Computer Science*, 8(1-2):1–141, 2012. doi:10.1561/0400000054.

[139] C. Wagner, W. Kinzelbach, and G. Wittum. Schur-complement multigrid. *Numerische Mathematik*, 75(4):523–545, 1997. doi:10.1007/s00211005.

[140] G. G. Walter and M. Contreras. *Compartmental Modeling with Networks*. Birkhäuser, 1999. doi:10.1007/978-1-4612-1590-5.

[141] C. Wang, A. Bernstein, J. Y. Le Boudec, and M. Paolone. Explicit conditions on existence and uniqueness of load-flow solutions in distribution networks. *IEEE Transactions on Smart Grid*, 9(2):953–962, 2018. doi:10.1109/TSG.2016.2572060.

[142] C. Wang and Y. Tokad. Polygon to star transformations. *IRE Transactions on Circuit Theory*, 8(4):489–491, 1961. doi:10.1109/TCT.1961.1086831.

[143] J. B. Ward. Equivalent circuits for power-flow studies. *Transactions of the American Institute of Electrical Engineers*, 68(1):373–382, 2009. doi:10.1109/EE.1949.6444973.

[144] L. Weinberg. *Network Analysis and Synthesis*. R.E. Krieger Pub. Co., 1975.

[145] J. D. Weston. Unification of linear network theory. *Journal of the British Institution of Radio Engineers*, 6(1):4, 1946. doi:10.1049/jbire.1946.0002.

[146] S. Wiggins. *Introduction to Applied Nonlinear Dynamic Systems and Chaos*. Texts in Applied Mathematics. Springer, 2nd edition, 2003.

[147] J. C. Willems. Dissipative dynamical systems–Part I: General theory. *Archive for Rational Mechanics and Analysis*, 45(5):321–351, 1972. doi:10.1007/BF0027649.

[148] J. C. Willems. Paradigms and puzzles in the theory of dynamical systems. *IEEE Transactions on Automatic Control*, 36(3):259–294, 1991. doi:10.1109/9.73561.

[149] J. C. Willems. Terminals and ports. *IEEE Circuits and Systems Magazine*, 10(4):8–26, 2010. doi:10.1109/MCAS.2010.938635.

[150] J. C. Willems and E. I. Verriest. The behavior of resistive circuits. In *IEEE Conf. on Decision and Control and Chinese Control Conference*, pages 8124–8129, Shanghai, China, December 2009. doi:10.1109/CDC.2009.5400390.

[151] A. N. Willson. On the solutions of equations for nonlinear resistive networks. *Bell System Technical Journal*, 47(8):1755–1773, 1968. doi:10.1002/j.1538-7305.1968.tb00101.x.

[152] C. W. Wu and L. O. Chua. Application of Kronecker products to the analysis of systems with uniform linear coupling. *IEEE Transactions on Circuits and Systems I: Fundamental Theory and Applications*, 42(10):775–778, 1995. doi:10.1109/81.473586.

[153] W. Xia and M. Cao. Analysis and applications of spectral properties of grounded Laplacian matrices for directed networks. *Automatica*, 80:10–16, 2017. doi:10.1016/j.automatica.2017.01.009.

[154] W. Xiao and I. Gutman. Resistance distance and Laplacian spectrum. *Theoretical Chemistry Accounts*, 110(4):284–289, 2003. doi:10.1007/s00214-003-0460-4.

[155] L. Yen, M. Saerens, and F. Fouss. A link-analysis extension of correspondence analysis for mining relational databases. *IEEE Transactions on Knowledge and Data Engineering*, 23(4):481–495, 2011. doi:10.1109/TKDE.2010.142.

[156] G. F. Young, L. Scardovi, and N. E. Leonard. Robustness of noisy consensus dynamics with directed communication. In *American Control Conference*, pages 6312–6317, Baltimore, MD, USA, 2010. doi:10.1109/ACC.2010.5531506.

[157] G. F. Young, L. Scardovi, and N. E. Leonard. A new notion of effective resistance for directed graphs – Part I: Definition and properties. *IEEE Transactions on Automatic Control*, 61(7):1727–1736, 2016. doi:10.1109/TAC.2015.2481978.

[158] S. Yu, H. D. Nguyen, and K. S. Turitsyn. Simple certificate of solvability of power flow equations for distribution systems. In *IEEE Power & Energy Society General Meeting*, pages 1–5, Denver, CO, USA, July 2015. doi:10.1109/PESGM.2015.7286371.

[159] C. Zhang, D. Florêncio, and P. A. Chou. Graph signal processing–a probabilistic framework. *Microsoft Research, Redmond, WA, USA, Tech. Rep. MSR-TR-2015-31*, 2015.

[160] F. Zhang. *The Schur Complement and Its Applications*. Springer, 2005.

[161] K. Zhou, J. C. Doyle, and K. Glover. *Robust and Optimal Control*. Prentice Hall, 1996.

[162] D. Zonetti, R. Ortega, and A. Benchaib. Modeling and control of HVDC transmission systems from theory to practice and back. *Control Engineering Practice*, 45:133–146, 2015. doi:10.1016/j.conengprac.2015.09.012.

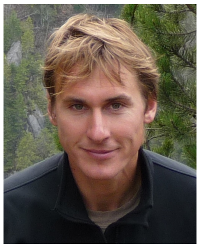

Florian Dörfler (S'09–M'13) is an Assistant Professor at the Automatic Control Laboratory at ETH Zürich. He received his Ph.D. degree in Mechanical Engineering from the University of California at Santa Barbara in 2013, and a Diplom degree in Engineering Cybernetics from the University of Stuttgart in 2008. From 2013 to 2014 he was an Assistant Professor at the University of California Los Angeles. His primary research interests are centered around distributed control, complex networks, and cyber-physical systems currently with applications in energy systems and smart grids. His students were winners or finalists for Best Student Paper awards at the European Control Conference (2013), and the American Control Conference (2016), and the PES PowerTech Conference 2017. His articles received the 2010 ACC Student Best Paper Award, the 2011 O. Hugo Schuck Best Paper Award, and the 2012-2014 Automatica Best Paper Award, and the 2016 IEEE Circuits and Systems Guillemin-Cauer Best Paper Award. He is a recipient of the 2009 Regents Special International Fellowship, the 2011 Peter J. Frenkel Foundation Fellowship, and the 2015 UCSB ME Best PhD award.

John W. Simpson-Porco (S'11–M'16) received the B.Sc. degree in Engineering Physics from Queen's University, Kingston, ON, Canada in 2010, and the Ph.D. degree in Mechanical Engineering from the University of California at Santa Barbara, Santa Barbara, CA, USA in 2015. He is currently an Assistant Professor of Electrical and Computer Engineering at the University of Waterloo, Waterloo, ON, Canada. He was previously a visiting scientist with the Automatic Control Laboratory at ETH Zürich, Zürich, Switzerland. His research focuses on the control and optimization of multi-agent systems and networks, with applications in modernized power grids. Prof. Simpson-Porco is a recipient of the 2012–2014 IFAC Automatica Prize and the Center for Control, Dynamical Systems and Computation Best Thesis Award and Outstanding Scholar Fellowship.

Francesco Bullo (S'95-M'99-SM'03-F'10) is a Professor with the Mechanical Engineering Department and the Center for Control, Dynamical Systems and Computation at the University of California, Santa Barbara. He was previously associated with the University of Padova, the California Institute of Technology, and the University of Illinois. His research interests focus on network systems and distributed control with application to robotic coordination, power grids and social networks. He is the coauthor of Geometric Control of Mechanical Systems (Springer, 2004) and Distributed Control of Robotic Networks (Princeton, 2009); his forthcoming "Lectures on Network Systems" is available on his website. He received best paper awards for his work in IEEE Control Systems, Automatica, SIAM Journal on Control and Optimization, IEEE Transactions on Circuits and Systems, and IEEE Transactions on Control of Network Systems. He is a Fellow of IEEE and IFAC. He has served on the editorial boards of IEEE, SIAM, and ESAIM journals, and will serve as IEEE CSS President in 2018.